ORNL-5442

Dynamic and Static Measurements of Elastic Constants with Data on 2¼ Cr-1 Mo Steel, Types 304 and 316 Stainless Steels, and Alloy 800H

J. P. Hammond
L. T. Ratcliff
C. R. Brinkman
M. W. Moyer
C. W. Nestor, Jr.

[redacted]

OAK RIDGE NATIONAL LABORATORY
CENTRAL RESEARCH LIBRARY
CIRCULATION SECTION
4500N ROOM 175
LIBRARY LOAN COPY
DO NOT TRANSFER TO ANOTHER PERSON
If you wish someone else to see this report, send in name with report and the library will arrange a loan.
UCN-7969 (3 9-77)

OAK RIDGE NATIONAL LABORATORY
OPERATED BY UNION CARBIDE CORPORATION · FOR THE DEPARTMENT OF ENERGY

Printed in the United States of America. Available from
the Department of Energy,
Technical Information Center
P.O. Box 62, Oak Ridge, Tennessee 37830
Price: Printed Copy $5.25; Microfiche $3.00

This report was prepared as an account of work sponsored by an agency of the United States Government. Neither the United States Government nor any agency thereof, nor any of their employees, contractors, subcontractors, or their employees, makes any warranty, express or implied, nor assumes any legal liability or responsibility for any third party's use or the results of such use of any information, apparatus, product or process disclosed in this report, nor represents that its use by such third party would not infringe privately owned rights.

ORNL-5442
Distribution
Category UC-79b, -h, -k

Contract No. W-7405-eng-26

Metals and Ceramics Division

DYNAMIC AND STATIC MEASUREMENTS OF ELASTIC CONSTANTS WITH DATA ON 2 1/4 Cr-1 Mo STEEL, TYPES 304 AND 316 STAINLESS STEELS, AND ALLOY 800H

J. P. Hammond L. T. Ratcliff C. R. Brinkman
M. W. Moyer C. W. Nestor, Jr.

Date Published: February 1979

OAK RIDGE NATIONAL LABORATORY
Oak Ridge, Tennessee 37830
operated by
UNION CARBIDE CORPORATION
for the
DEPARTMENT OF ENERGY

CONTENTS

	Page
ABSTRACT	1
INTRODUCTION	1
MATERIALS	2
TEST METHODS	5
Dynamic Method	5
Static Methods	7
Tests With LVDT Gages	11
Tests With Weldable Resistance Gages	13
Tests With Capacitive Gages	15
EXPERIMENTAL RESULTS	19
2 1/4 Cr-1 Mo Steel	25
Type 304 Stainless Steel	29
Type 316 Stainless Steel	31
Alloy 800H	33
DISCUSSION OF RESULTS	35
SUMMARY AND CONCLUSIONS	39
ACKNOWLEDGMENTS	41
APPENDIX A — CALCULATIONS OF DYNAMIC ELASTIC CONSTANTS	42
APPENDIX B — RELATIONS BETWEEN ISOTROPIC ELASTIC CONSTANTS	46
APPENDIX C — ELECTRICAL CIRCUITS OF THE WELDABLE RESISTANCE GAGES	47

DYNAMIC AND STATIC MEASUREMENTS OF ELASTIC CONSTANTS WITH DATA ON 2 1/4 Cr-1 Mo STEEL, TYPES 304 AND 316 STAINLESS STEELS, AND ALLOY 800H[1]

J. P. Hammond L. T. Ratcliff C. R. Brinkman
M. W. Moyer[2] C. W. Nestor, Jr.[3]

ABSTRACT

Methods for determining the dynamic and static elastic constants (E, G, and ν) of engineering materials were developed and evaluated. A hybrid sonic method incorporating the double pulse, block-sample technique for determining accurate room-temperature data and the single pulse, thin-wire technique for gathering elevated-temperature data were used to determine the dynamic elastic constants. Of three methods examined for measuring static constants (using the linear variable differential transformer, the weldable resistance gage, and the capacitive gage), the method employing the linear variable differential transformer gage served well as a reference method for determining Young's modulus. The method using the capacitive gage showed greatest merit for determining combined E, G, and ν.

The dynamic and static elastic constants of 2 1/4 Cr-1 Mo steel, types 304 and 316 stainless steel, and alloy 800H were determined from room temperature to 649°C (1200°F) and higher. These data are expressed as cubic polynomials, which proved easy to use and effective for recording results. Expected values of the elastic constants as functions of temperature are computed with the polynomial and correlated with contemporary data.

INTRODUCTION

Elastic constants are of great importance in engineering design and structural verification work. Also, they are used in the theoretical and applied fields of physical metallurgy. Too often data on elastic

[1]Work performed under DOE/RRT 189a OH050, "Mechanical Properties for Structural Materials," and 189a OH028, "Steam Generator Materials Development."

[2]Development Division, Oak Ridge Y-12 Plant.
[3]Computer Sciences Division.

constants are unavailable, inaccurate, or determined under inadequately documented conditions.

Precise measurements show that the elastic stress-strain relationships for metals are not perfectly linear and become progressively more nonlinear as strain increases. At the higher levels of strain, measurements reveal evidence of incipient plastic behavior, with strain a function of instantaneous stress, time, temperature, and prior strain history. At temperatures where thermally activated processes occur, inelastic strain may become a factor even at low stress levels. As a consequence, discrepancies sometimes occur between elastic constants determined at different strain levels and rates of strain or between constants established by the dynamic (sonic) and static methods. Where the static and dynamic values differ the modulus employed in design should be established in relation to the specific application, giving appropriate consideration to the conditions of strain.

In studies sponsored by the breeder reactor program, improved techniques for determining both dynamic and static constants were developed, and data for a variety of structural materials were established and reported in ORNL project progress reports. The purpose of this report is to present the dynamic and static Young's modulus (E), shear modulus (G), and Poisson's ratio (ν) of 2 1/4 Cr-1 Mo steel, types 304 and 316 stainless steel, and alloy 800H for 24 to 705°C (75 to 1300°F) or higher and correlate these results with the more significant data of the literature. Because the instrumentation and techniques used to gather this information in many respects are new, they are evaluated and documented.

MATERIALS

Table 1 lists the materials examined with heat number, product form, dimensions, specification, and metal condition and gives the method of test and test temperature range. The chemical analyses of the alloys are given in Table 2. All conform to their respective ASTM specifications.

Table 1. Materials

Alloy	Heat	Form	Dimensions (mm)	Dimensions (in.)	ASTM Specification	Specimen Condition	Test Type	Test Range, RT to (°C)	Test Range, RT to (°F)
2 1/4 Cr–1 Mo	20017	Plate	25	1	A 387-76, Gr. 22	IA[a]	Dynamic	649	1200
2 1/4 Cr–1 Mo	20017	Plate	25	1	A 387-76, Gr. 22	IA[a]	Static	704	1300
Type 304 stainless steel	9T2796	Plate	25	1	A 240-75a	SA[b]	Dynamic	871	1600
Type 304 stainless steel	9T2796	Plate	25	1	A 240-75a	SA[b]	Static	871	1600
Type 304 stainless steel	60551	Bar	127 × 178	5 × 7	A 240-75a	SA[b]	Dynamic	871	1600
Type 304 stainless steel	346544	Plate	51	2	A 240-75a	SA[b]	Dynamic	871	1600
Type 316 stainless steel	8092297	Plate	25	1	A 240-75a	SA[b]	Dynamic	871	1600
Alloy 800H	HH6758A	Plate	30	1.2	B 409-74a	SA[c]	Dynamic	899	1650

Note: Test specimens were taken with axes parallel to rolling direction from central locations. RT = room temperature. IA = isothermally annealed; SA = solution annealed.

[a]Austenitized at 727 ± 14°C, cooled to 704 ± 14°C at <83°C/h, held for 2 h and cooled to 24°C at <6°C/min.

[b]Heated 0.5 h at 1065°C.

[c]Heated 1 h at 1149°C.

Table 2. Chemical Analyses

Heat Symbol	Chemical Element, wt %																					
	C	N	P	B	O	H	Ni	Mn	Cr	Si	Mo	S	Nb	V	Ti	Ta	W	Cu	Co	Pb	Sn	Al
										2 1/4 Cr-1 Mo Steel												
0017	0.135		0.012				0.16	0.57	2.2	0.37	0.92	0.016										
										Type 304 Stainless Steel												
2796	0.047	0.031	0.029		0.0110	0.006	9.58	1.22	18.5	0.47	0.10	0.012	0.008	0.037	0.003	<0.0005	0.022	0.10	0.05	0.01	0.02	
0551	0.043	0.017	0.022	0.0010	0.0220	0.0013	9.40	1.20	18.5	0.59	0.30	0.018	0.0140	0.050	0.025	<0.0050	0.049	0.25	0.08	0.01	0.01	
6544	0.063	0.019	0.023	0.0002	0.0081	0.0006	9.12	0.99	18.4	0.47	0.2	0.006	0.0050	0.025	0.017	0.0006	0.026	0.12	0.05	0.01	0.01	
										Type 316 Stainless Steel												
2297	0.065	0.031	0.022	0.0005	0.0043	0.0007	13.9	1.88	16.5	0.51	2.4	0.018	0.0004		<0.01	0.1	0.020	0.12	0.01	<0.02	<0.02	
										Alloy 800H												
758A	0.08						32.31	0.92	20.19	0.40		0.004			0.34			0.74				0.16

TEST METHODS

The dynamic and static constants were established and recorded as a function of temperature using a cubic polynomial. This model proved effective in representing the data and is easy to use.[4] The equation combines an accurate room-temperature (RT) value of the constant with elevated temperature data of less absolute accuracy but high relative accuracy. The model has the desirable feature of intersecting the RT value of the constant:

$$X = X_0[1 + A(T - T_0) + B(T - T_0)^2 + C(T - T_0)^3] \ , \qquad (1)$$

where

X = the property (E, G, or ν) at T,
X_0 = same at RT,
T = temperature in °C,
T_0 = RT, and
A, B, and C = constants.

Because good values of X_0 lend accuracy to data predicted at elevated temperature, the RT data on which X_0 is based generally are established by more painstaking procedures. The polynomial is fitted to the total data by the least squares method in a computer by optimizing A, B, and C. Thus, the elastic property as a function of temperature may be expressed by specifying these three coefficients along with X_0. The goodness of fit of the model to the data generally is given by the standard deviation.

Dynamic Method

Although the dynamic (sonic) method of test was fully described previously,[5] its essential details are given here.

---

[4]J. P. Hammond, M. W. Moyer, and C. R. Brinkman, "Effects of Materials and Test Variables on Elastic Constants of 2 1/4 Cr-1 Mo Steel and Type 304 Stainless Steel," pp. 1037-41 in *Proc. 2nd Int. Conf. Mechanical Behavior of Materials*. American Society for Metals, Metals Park, Ohio, 1976.

[5]M. W. Moyer and J. P. Hammond, *Ultrasonic Measurement of Elastic Constants at Temperatures from 24 to 1100°C*, Y-2047 (September 1976).

Accurate room-temperature values of the constants were established by a double-pulse, block-sample method similar to the pulse-echo technique of Papadakis.[6] The technique uses an oscillator with gating circuitry that allows two successive oscillations to trigger the transducer. The frequency of the oscillator is adjusted to obtain superposition of multiple reflections in the sample caused by two excitation pulses. A counter measures the oscillator frequency, from which transit time and, hence, the sound velocity is established. Sound waves of the longitudinal and shear modes at a frequency of 5 MHz were employed on two test specimens of 6.5 and 13-mm thickness.

Corrections were made for the usual systematic errors of the method by techniques similar to Papadakis.[7] Errors from phase shifts at the transducer bond and electronic delays in the circuit were corrected by using measurements on the two samples in conjunction with a zero-thickness-offset technique.[5] Room-temperature values of the elastic constants (X_0) with standard errors of reproducibility of from 0.1 to 0.4% were obtained by averaging several measurements.

The elevated-temperature dynamic data were gatherd by a thin-wire method similar to that of Brown.[8] Extensional and torsional sound waves of 0.1 to 0.2 MHz were introduced in specimens measuring about 2.5 mm diam by 100 mm long and contained in an electric furnace. The waves were introduced remotely through an intermediate buffer rod with a magnetostrictive transducer. Two cyclic runs were made to peak temperature, giving a total of about 120 data points. The data, recorded automatically, were analyzed and plotted with a two-program package in a PDP-15/20 and a PDP-15/35 computer.

The equations used to calculate the various dynamic elastic constants from the velocity data[5] are given in Appendix A. The methods used for

---

[6]E. P. Papadakis, "Ultrasonic Phase Velocity by the Pulse-Echo-Overlap Method Incorporating Diffraction Phase Corrections," *J. Accoust. Soc. Am.* 42: 1045-51 (1967).

[7]E. P. Papadakis, "Absolute Accuracy of the Pulse-Echo Overlap Method and the Pulse-Superposition Method for Ultrasonic Velocity," *J. Accoust. Soc. Am.* 52: 843-46 (1972).

[8]H. L. Brown and P. E. Armstrong, "Young's Modulus Measurements Above 2000°C," *Rev. Sci. Instrum.* 34(6): 636-39 (June 1963).

computing the standard deviations of the constants are included. The Young's modulus and shear modulus were determined directly from the velocity data, whereas Poisson's ratio was derived from E and G by the basic relationship:

$$\nu = -1 + E/2G \ . \tag{2}$$

The foregoing methods for establishing elastic constants assume isotropy of the test material, and for most polycrystalline structural materials this is valid. However, we measured the degree of anisotropy in the different test materials for the record. Two measurements of the shear velocity on the block sample were made with the polarization direction of the sound wave rotated 90° between measurements. The anisotropy value was taken as one-half the difference between the two velocities measured [Appendix A, Eq. (A23)].

Static Methods

The static elastic constants were determined by pulling specimens in tension in a 44.5-kN (10,000-lb) Instron tensile test machine and simultaneously measuring longitudinal extension (ε_l) and transverse contraction (ε_t) in syncronism with stress (σ). Signals of these parameters were fed into two x-y recorders, and the modulus values (E and ν) were determined by establishing slopes to appropriately plotted curves by the chord method (ASTM E 231-69). Young's modulus was equated with $\Delta\sigma/\Delta\varepsilon_l$ and Poisson's ratio with $-\Delta\varepsilon_t/\Delta\varepsilon_l$. The shear modulus was established from E and ν by the basic relationship:

$$G = E/2(1 + \nu) \ . \tag{3}$$

The remaining equations interrelating the various elastic constants of isotropic bodies are given in Appendix B.

The following three strain transducers were examined for monitoring strain:

1. linear variable differential transformer, type 6233, manufactured by Automatic Temperature Controls, Inc., King of Prussia, Pennsylvania;
2. weldable resistance strain gage, model MG-425, manufactured by AILTECH Corporation, City of Industry, California;
3. capacitive strain gage, model HTC-DC-100, made by HITEC Corporation, Westford, Massachusetts.

Stress was sensed with a conventional full-bridge, resistance gage load cell (Instron make) mounted at the base of the load train. A universal joint was incorporated both above and below the test specimen to aid stress alignment. The current ASTM specification on practices and standards governing tension testing (E 8-69 and E 74-64), extensometers (E 83-67), and resistance strain gages (E 251-67) were adhered to.

The static elastic constants were determined by a new technique, which employs a single test specimen repeatedly for gathering the elevated-temperature data, if not all the data. By doing this and taking care not to disturb the load train between test measurements, high resolution of data is assured. The influence of any accruing thermal-mechanical effects to the specimen is assessed with spot tests made on fresh specimens.[9] This information is then used to make any desirable adjustment to the modulus-temperature curve. The foregoing "repetitive" technique was dictated by the relatively high cost of the strain transducers employed, which in the case of the resistance and capacitive gages are expendable. On the other hand, the present method is time-saving in that a new specimen need not be loaded into the train with each measurement, as customarily is the case, and overall may be the more economical method.

Three additional features of our static test methods are noteworthy. First, to assure that strain is free of an inelastic component, testing was confined to very low levels of strain: 1.40×10^{-4} for the linear

[9]Performed with linear variable differential transformer transducers mounted on a detachable extensometer so as not to expend gages.

variable differential transformer (LVDT) and resistance gages and 1.00×10^{-4} for the capacitive gage. For the test temperatures used this generally gave reversible stress-strain graphs. Second, as will be noted subsequently from photographs showing the arrangement of gages on the respective test specimens, the principle of strain averaging was employed. By mounting gages at symmetrically opposite points about the specimen axis, correction for specimen bending and associated movement of the principal stress is achieved.[10] Finally, to minimize the influence of thermal strains, the temperature of the test specimens was controlled to very close limits during test (±0.15°C).

The equipment used for measuring the static elastic constants that is common to all three of the methods is illustrated in Figs. 1 through 3. Figure 1 shows the Instron tensile testing machine with its console to the left and the two x-y plotters (type 7045A Hewlett-Packard) in front. The load train of the machine in this particular instance contains the test specimen that incorporates capacitive gages (see Fig. 3 for blowup). The universal joints above and below the specimen and the load cell at the base of the train can be seen in Fig. 1.

The cabinet shown in Fig. 2 contains signal-treating circuits for the load cell and the three strain sensing systems. The modules housed in the rack at the top accommodate the load cell and the signals from the LVDT gages. The middle rack treats signals from the capacitive gages, while the bottom rack treats signals from the weldable resistance strain gages.

The electric furnace used to heat test specimens (Fig. 3) is resistance heated and opens at the side to accommodate the load train. It has three zones, powered individually with a Thermo Max Controller, to give temperature leveling. The controller was actuated with three Chromel vs Alumel thermocouples mounted at the center and the extremities of the specimen gage section.

---

[10]A. K. Schmieder, "Measuring the Apparatus Contribution to Bending in Tension Specimens," pp. 15-42 in *ELevated Temperature Testing Problem Areas, ASTM Spec. Tech. Publ.* 488, American Society for Testing and Materials, Philadelphia, 1971.

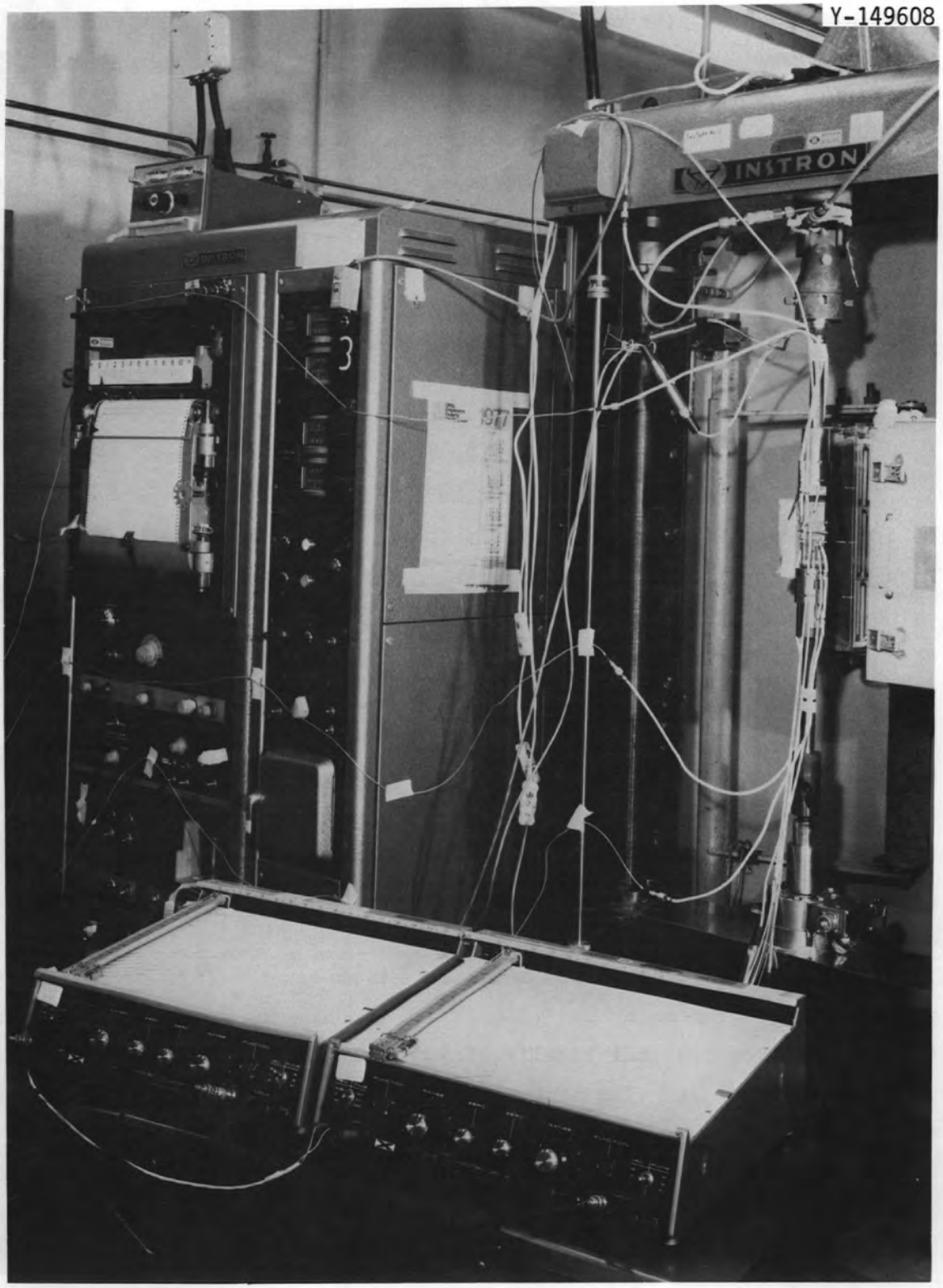

Fig. 1. Instron Tensile Test Machine and Associated Equipment for Measuring Elastic Constants.

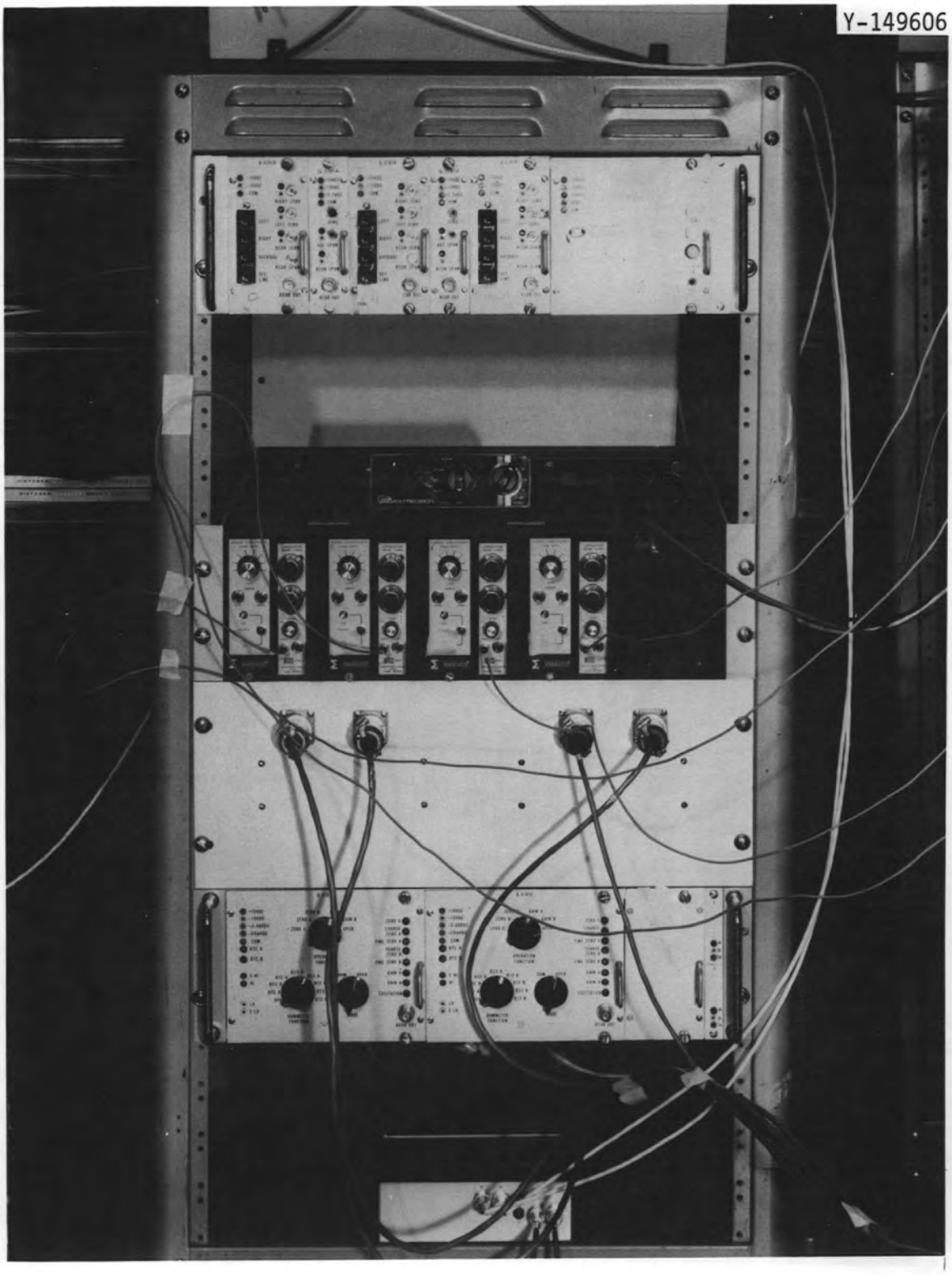

Fig. 2. Cabinet Containing Signal Treating Circuits for Strain Gages.

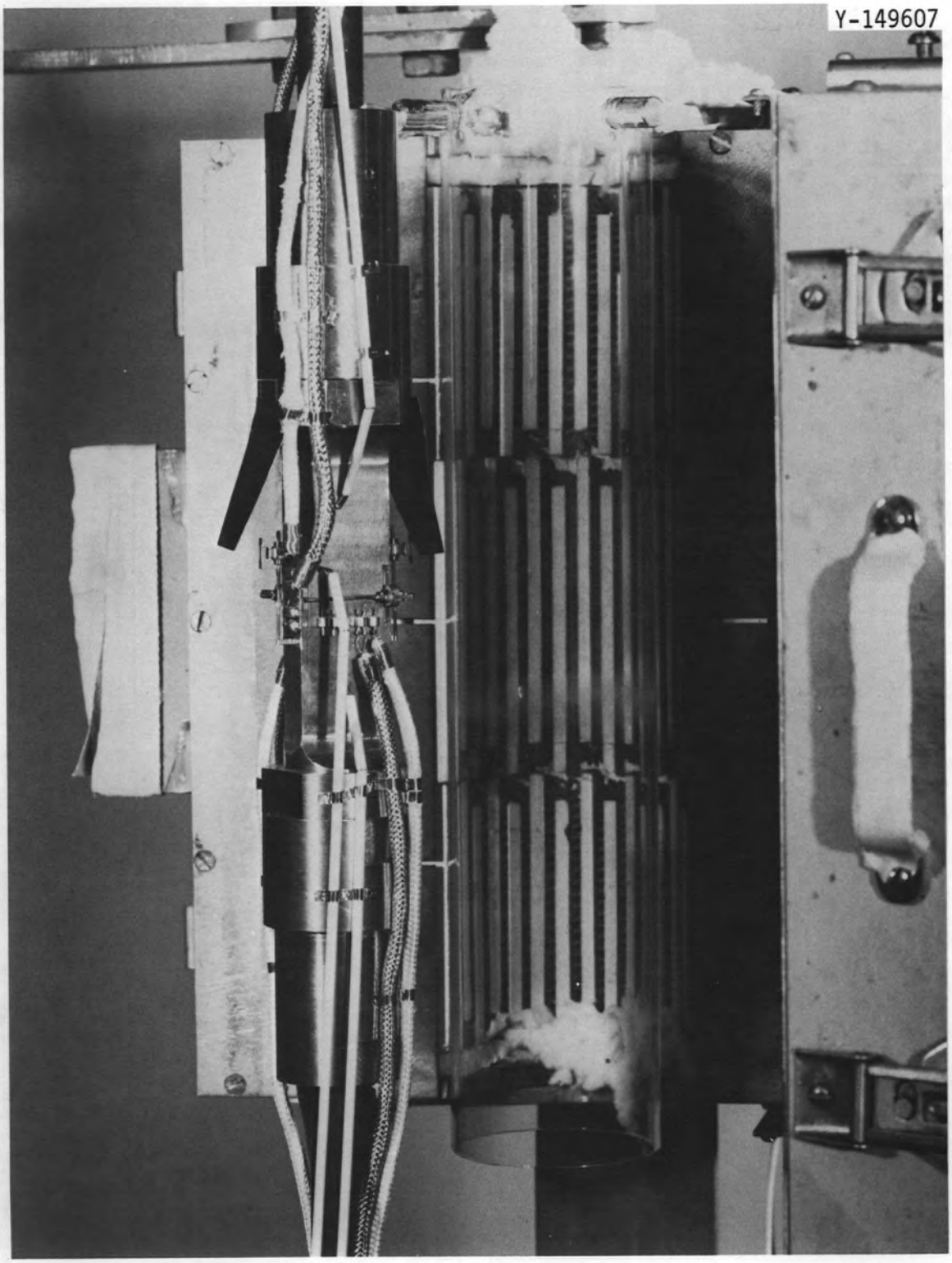

Fig. 3. Three-Phase Electrical Furnace Adjoining Load Train Containing the Specimen Equipped with Capacitive Gages.

Suspended to the side of the load train in Fig. 3 is a quartz cylinder used to contain a dynamic atmosphere of Ar-4% H_2 for protecting the test specimen during runs to elevated temperature. In use this, of course, mounts around the specimen. Spun glass caulking is used to help contain the protective gas.

Tests With LVDT Gages

Two type 6233 LVDT transducers remotely mounted on a conventional round-bar specimen [12.8-mm-diam by 5.1-mm (0.505- by 2.0-in.) gage] with a SETEC 800 series extensometer performed well for measuring Young's modulus to temperatures as high as 871°C (1600°F). The extensometer with integrated LDVT gages is shown mounted on the test specimen in Fig. 4. Means were not devised for determining ν or G with this gage. The extensometer places the LVDT gages outside the furnace since they are not constructed of heat-resistant materials, as are the other two gages.

Whereas the resistance and capacitive gages are once calibrated at manufacture by their supplier, the LVDT gages were readily calibrated on site. This was done routinely with a portable digital micrometer, model 1398, supplied by IKL, Inc. Whereas the specification for this unit prescribes a resolution of 10×10^{-6}, we obtained a resolution estimated at 2×10^{-6} by subdividing vernier divisions. Additional factors that contributed significantly to the success of the LVDT method are the following.

First, the particular LVDT model used was a special-order type offering high electrical sensitivity (0.6 mV output per volt excitation per micrometer displacement of the armature) as a result of very fine core and field windings. Second, means were provided for aligning and mounting the extensometer on the test specimen to a higher than ordinary degree of precision, as will be shown below. Finally, the extensometer was thermally stabilized during elevated-temperature test runs by a housing mounted at the base of the furnace to shield the lower extremity of the extensometer from external air currents. The latter measure proved important since such thermal effects produce gage strains as high as 25×10^{-6} over a period of just 15 min under the more adverse conditions.

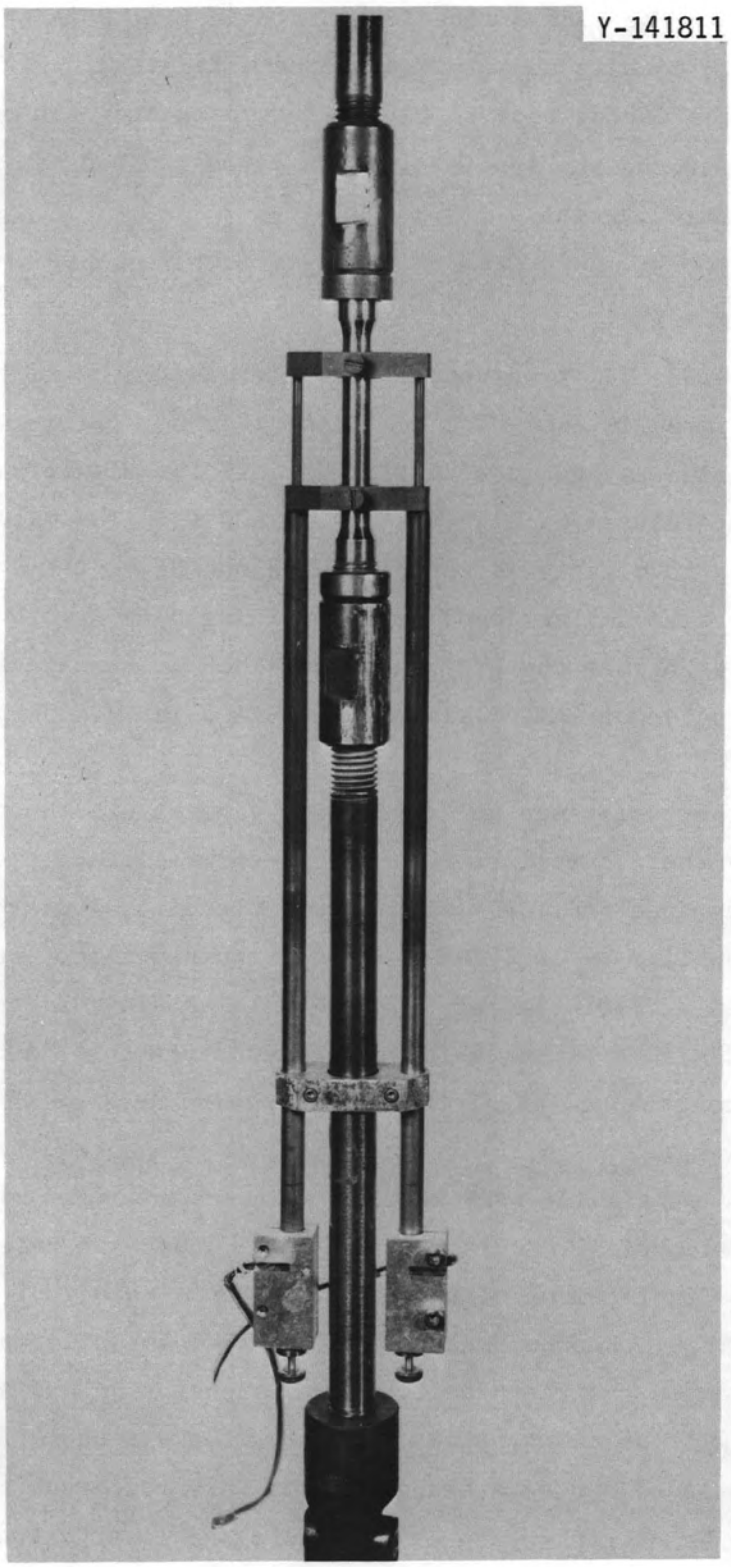

Fig. 4. Round Test Specimen Fitted with Extensometer Incorporating Two Type 6233 LVDT Gages.

Conical holes (three sets) in test specimens with which to mount the extensometer by means of set screws (Fig. 4) were incorporated and certified by the ORNL Inspection Engineering Department to the specification limits shown in Fig. 5. Whereas the tolerance shown for the gage length is not so unusual, the degree of alignment of the holes with the specimen axis is.

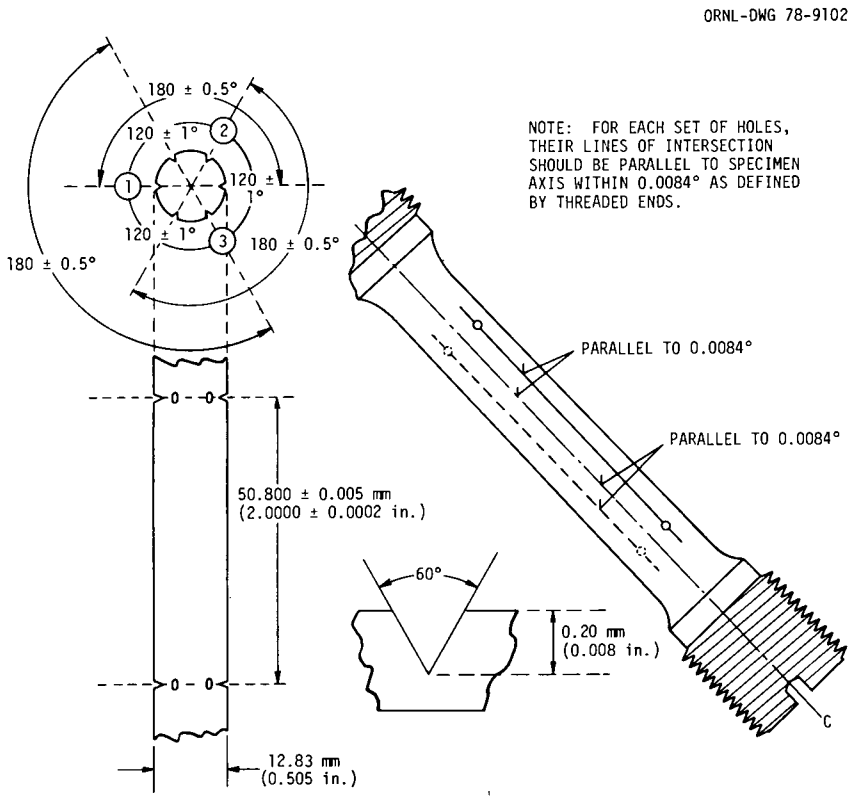

Fig. 5. Conical Holes in Gage of Round-Bar Specimen for Mounting Extensometer.

The foregoing LVDT test method was used as the reference means for establishing Young's modulus on all the structural materials. Additionally, it was used to establish the effects of repeated use of a single test specimen on the relationship of elastic constant with temperature.

The room-temperature E (X_0) values were established as an arithmetic mean of 72 total data points. For each of two test specimens and each of three azimuthal orientations about their axes (Fig. 5), four readings

were made each at the strain rates 0.1, 0.01, and 0.001/h. The elevated-temperature data were gathered by taking four readings at each of the same strain rates on the "repetitive" test specimen at each of the consecutive test temperatures (usually at 55°C intervals).

Tests With Weldable Resistance Gages

The subsize (12.7-mm-gage) weldable resistance gage, model MG-425, was evaluated comprehensively for our elastic constants application, making room- and elevated-temperature tests to 649°C (1200°F) on both 2 1/4 Cr-1 Mo steel and type 304 stainless steel. These gages, fitted to the stainless steel test specimen (of square cross-section measuring 15.5 mm on an edge) are illustrated in Fig. 6. The gages were aligned to high precision and spot-welded on the specimen by qualified procedures.

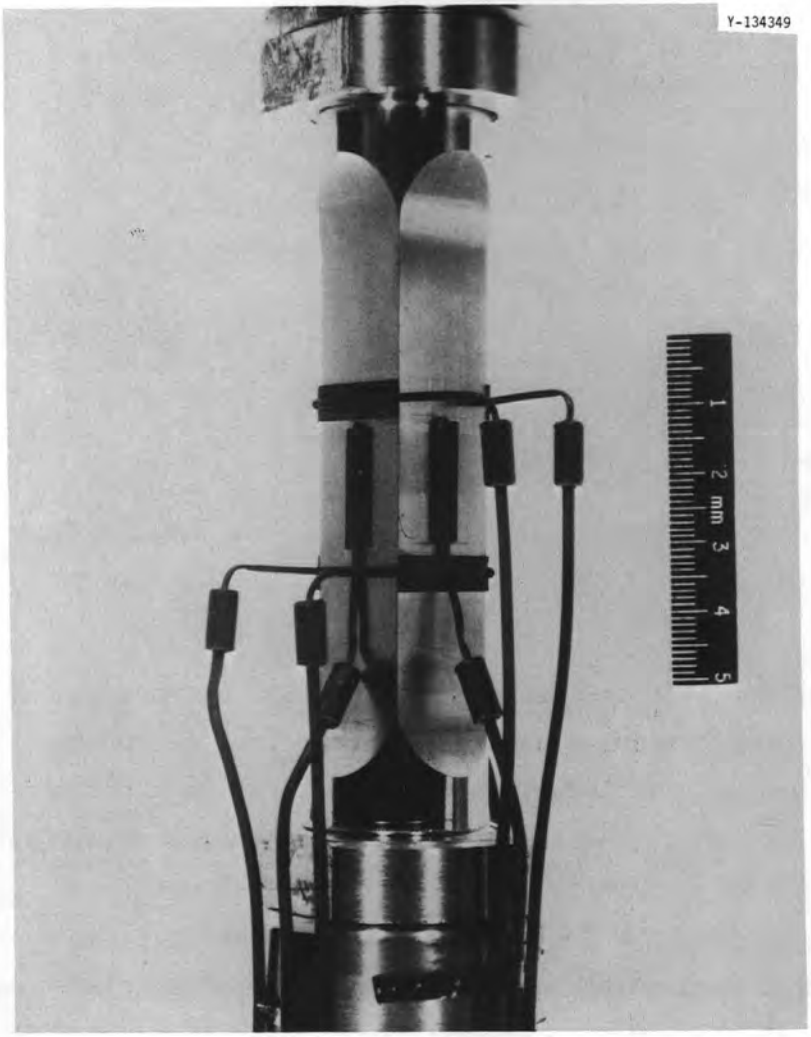

Fig. 6. Square Test Specimen Fitted with Eight Model MG-425 Resistance Strain Gages.

Two sets of two gages were mounted vertically and two sets horizontally for performing strain averaging and checking one set of gages against the other.

The particular gages employed were of the temperature-compensating type, which corrects for two sources of error in gage resistance: (1) resistance change resulting from differential thermal expansion between the active gage filament and the test specimen and (2) resistivity change in the active filament. The principles for making these corrections together with the circuits for averaging strain and treating signals before inputting to the plotters are given in Appendix C.

Whereas the standard SG-425 (25.4-mm gage) temperature-compensating gage has been reported[11,12] as giving satisfactory performance to 482°C (900°F), the 12.7-mm-gage version (MG-425) we employed failed to operate to the temperature limit and accuracy required for our work. For both the 2 1/4 Cr-1 Mo steel and the type 304 stainless steel the room-temperature compensation proved excessive at high temperatures. The latter problem appeared to be associated with the resistivity correction. As a result of the foregoing unresolved difficulties, the elastic constant data gathered with these gages are not reported here.

Tests With Capacitive Gages

The Boeing-type capacitive strain gage (model HTC-DC-100) was examined for our use because it is free of severe temperature errors and has a number of other attractive characteristics. It operates on the principle of differential capacitance and avoids the problem of differential expansion between gage and specimen by its linkup component being constructed of the test specimen material or a substitute of equivalent coefficient of thermal expansion. This is illustrated in the schematic drawing of the gage in Fig. 7.

---

[11] M. M. Lemcoe, "Errors in High-Temperature Strain Measurements," *Exp. Mech.* 3(2): 1-8 (February 1963).

[12] J. P. Gibbs, "Two Types of High-Temperature Weldable Strain Gages: Ni-Cr Half-Bridge Filaments and Pt-W Half-Bridge Filaments," *Exp. Mech.* 7(8): 19A-26A (August 1967).

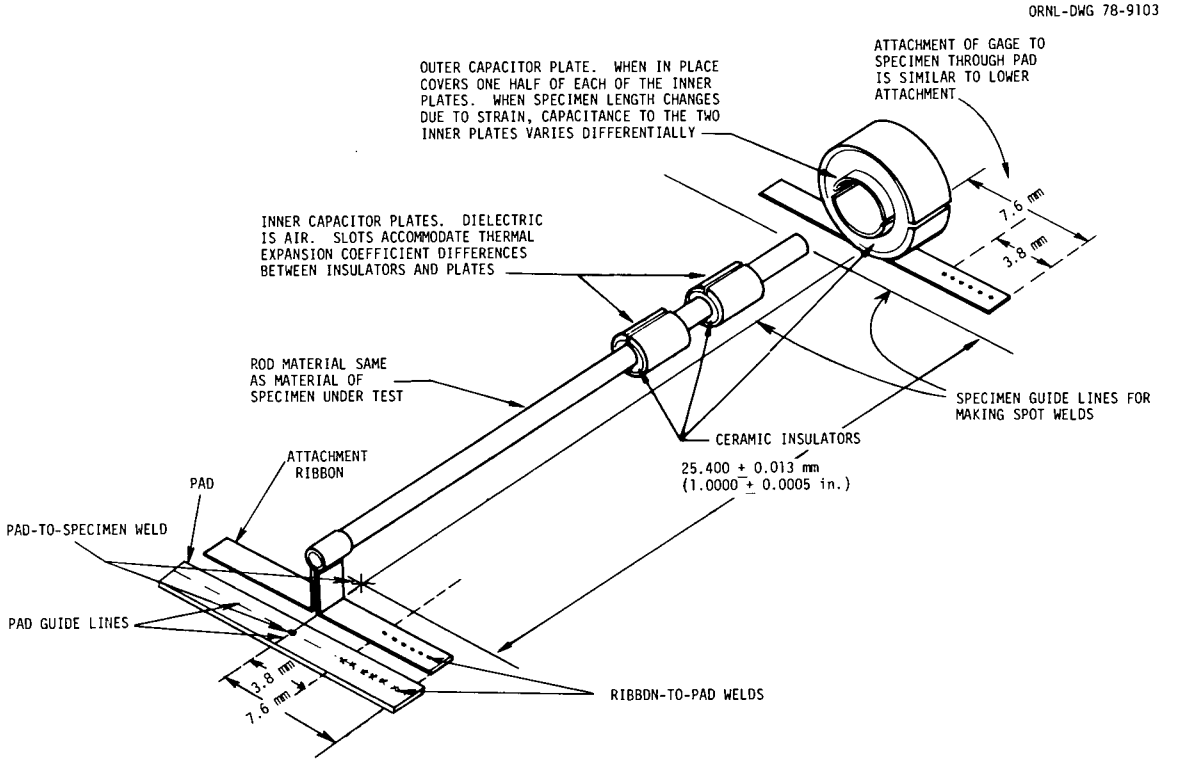

Fig. 7. Schematic of Boeing Capacitive Strain Gage and Attachment.

The strain-measuring system (except for plotters) of this method of test was supplied by HITEC, along with four capacitive gages. It consisted of the following items:

1. four signal conditioners, model 44.70;
2. four capacitive mode cards, model 4479.6;
3. two commoning boxes (special unit);
4. one rack adaptor, 115 V, model 4942; and
5. four sets each of types HTB and RTB cables.

The posts of the gages were fabricated of René 41, which is close to the material tested (2 1/4 Cr-1 Mo steel) in coefficient of thermal expansion. The equipment was operated to company instructions and certified gage factors.

The manufacturer's specifications for the gages and their associated strain measuring system are given in Table 3. Features of the system

Table 3. Specifications of Model HTC-DC-100 Capacitive Gage and Associated Equipment

Strain Gage	
Overall size (mm):	15 wide × 9 high × 32 long
Gage length (mm):	25.4 nominal
Maximum strain range:	±0.02
Loading:	80 g for 0.02 strain
Temperature range:	to 615°C
Sensitivity:	0.018 pF/0.001 (nominal)
Sensitivity change with temperature:	±4% at 615°C
Strain Measuring System (with dc supply set at 30 V)	
Nonlinearity: (Zero Based)	±0.5% to 0.003 at 24°C
	±1% to 0.0015 at 615°C
	±2% to 0.02 at 24°C
Drift:	0.003 max in 4 h with gage at 649°C
Resolution:	0.3% of min full scale of 0.0015 (including HP x-y plotter)
Thermal output: (Apparent strain)	+0.0003 to 615°C
Strain rate:	<2% nonlinearity to 0.03/s at 24°C
Carrier excitation:	6.5 to 7.0 V rms
Carrier frequency:	3.39 kHz
Output voltage:	±5 V dc max
Output current:	±5 mA max
Output impedance	Less than 1.0 Ω

important to us are (1) wide use-temperature range, (2) high signal linearity at reasonably good sensitivity, and (3) comparatively low thermal drift.

The capacitive gage test specimen, which measured 28 by 15.5 mm in cross section, is shown in Fig. 8. It again embodies strain averaging, with two gages mounted vertically and two horizontally. The gages were aligned by precise guidelines inscribed by the ORNL Inspection Engineering

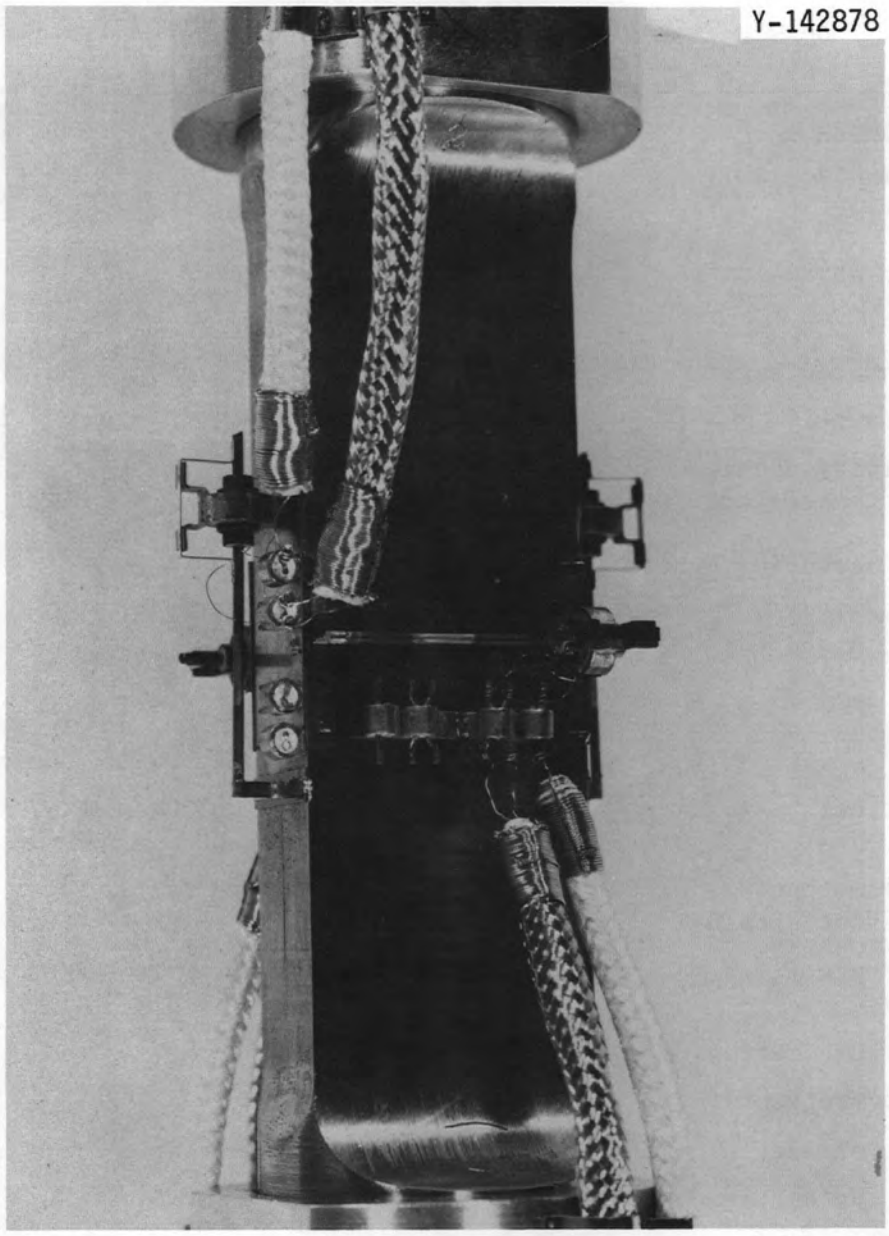

Fig. 8. Rectangular Test Specimen Fitted with Four Model HTC-DC-100 Capacitive Strain Gages.

Division and spot-welded on by a special attachment scheme to enable assessment of the individual gage lengths to high accuracy. The attachment method, which is illustrated in Fig. 7, consisted of the following. First, intermediate pads were fastened to the specimen by a single spot weld. Then the gage was attached by multiple spot-welding the gage

ribbons to the pads. A traversing digital microscope was used in conjunction with a destructive metallographic technique for delineating the weld nuggets to establish final gage lengths to an accuracy estimated to be about 0.05% (±0.013 mm).

Numerous additional problems required solution before the equipment performed satisfactorily, chief among which were the following. First, to remove pronounced background noise, electronic filters (1-5 Hz Butterworth low-pass modules) were inserted between the HITEC signal treating circuits and the x-y plotters. Second, the ac magnetic fields generated by the heating coils of the furnace interfered with the capacitance signals of the gages. This was remedied by inserting a 0.1-mm-thick type 304 stainless steel foil on the inner surface of the quartz cylinder that surrounded the specimen (Fig. 3). Third, metal shields needed to be welded on the specimen grips just above the vertical gages to protect their capacitors from falling debris (Fig. 3). Finally, to ensure stability of strain signals, the excitation and signal leads had to be well separated where they join to the gage terminals and kept motionless over their entire length during test.

With these modifications, consistent graphs of stress and transverse contraction as functions of longitudinal extension were obtained with minimal background noise. As will be seen subsequently, the Young's modulus curve for this method (2 1/4 Cr-1 Mo steel) agreed well with that obtained by the reference LVDT method. However, the Poisson's ratio values ran consistently high by about 18%. This was attributed to slight damage that occurred to one of the horizontal strain gages during shakedown testing. Consequently, our dynamic value of the RT ν (X_0) was used instead of the capacitive gage value to establish the polynomial model of ν by this method. As will be discussed subsequently, comparatively little difference should exist between the dynamic and static values of ν, and the substitution is warranted.

Static elastic constants (E, G, and ν) were determined for 2 1/4 Cr-1 Mo steel by the capacitive gage method from RT to 704°C (1300°F). Room-temperature E (X_0) was based on a total of 12 determinations consisting of six readings each at 0.01 and 0.001/h. Young's modulus and ν at elevated temperatures were based on eight determinations consisting of four each at 0.01 and 0.001/h.

Typical stress-strain graphs developed on 2 1/4 Cr-1 Mo steel at room temperature by the LVDT and capacitive gage methods for determining Young's modulus are compared in Fig. 9. Negligible hysteresis was evident in the graphs by either of the methods, and the strain was reversible. Observe that the curves of the LVDT system are perfectly smooth, whereas those developed with capacitive gages still show a moderate amount of background noise. This, however, did not appear to present a serious problem in assessing slopes.

EXPERIMENTAL RESULTS

The coefficients and X_0 values of cubic polynomials [Eq. (1)] required for computing the dynamic and static elastic constants (E, G, and ν) of 2 1/4 Cr-1 Mo steel, types 304 and 316 stainless steel, and alloy 800H as functions of temperature are recorded in Table 4. The computed dynamic constants of 2 1/4 Cr-1 Mo steel are given in Table 5, whereas the computed static constants of 2 1/4 Cr-1 Mo steel are given in Table 6 (capacitive gage and LVDT for E only). The computed dynamic elastic constants of type 304 stainless steel (heat 9T2796) are given in Table 7 along with the computed static constants (LVDT, for E only). Finally, the computed dynamic elastic constants for type 316 stainless steel and alloy 800H are recorded in Tables 8 and 9, respectively.

Before we interpret these results material by material, two Young's modulus-temperature curves established by the "repetitive" specimen technique (with LVDT gages) will be presented and the validity of results obtained by this method discussed. Figures 10 and 11 show the static E curves determined by this method for 2 1/4 Cr-1 Mo steel and type 304 stainless steel, respectively. Both curves are computer plotted. The standard error limits given in the graphs indicate that the polynomial models closely fit the data. The circles are values of Young's modulus established on "fresh" specimens. In establishing these values a bias correction factor was applied to correct for stress misalignment.[13]

---

[13]J. P. Hammond, "Elastic Constants of Engineering Construction Materials," *Mechanical Properties Test Data for Structural Materials Quart. Prog. Rep. April 30, 1976*, ORNL-5112, pp. 76-80.

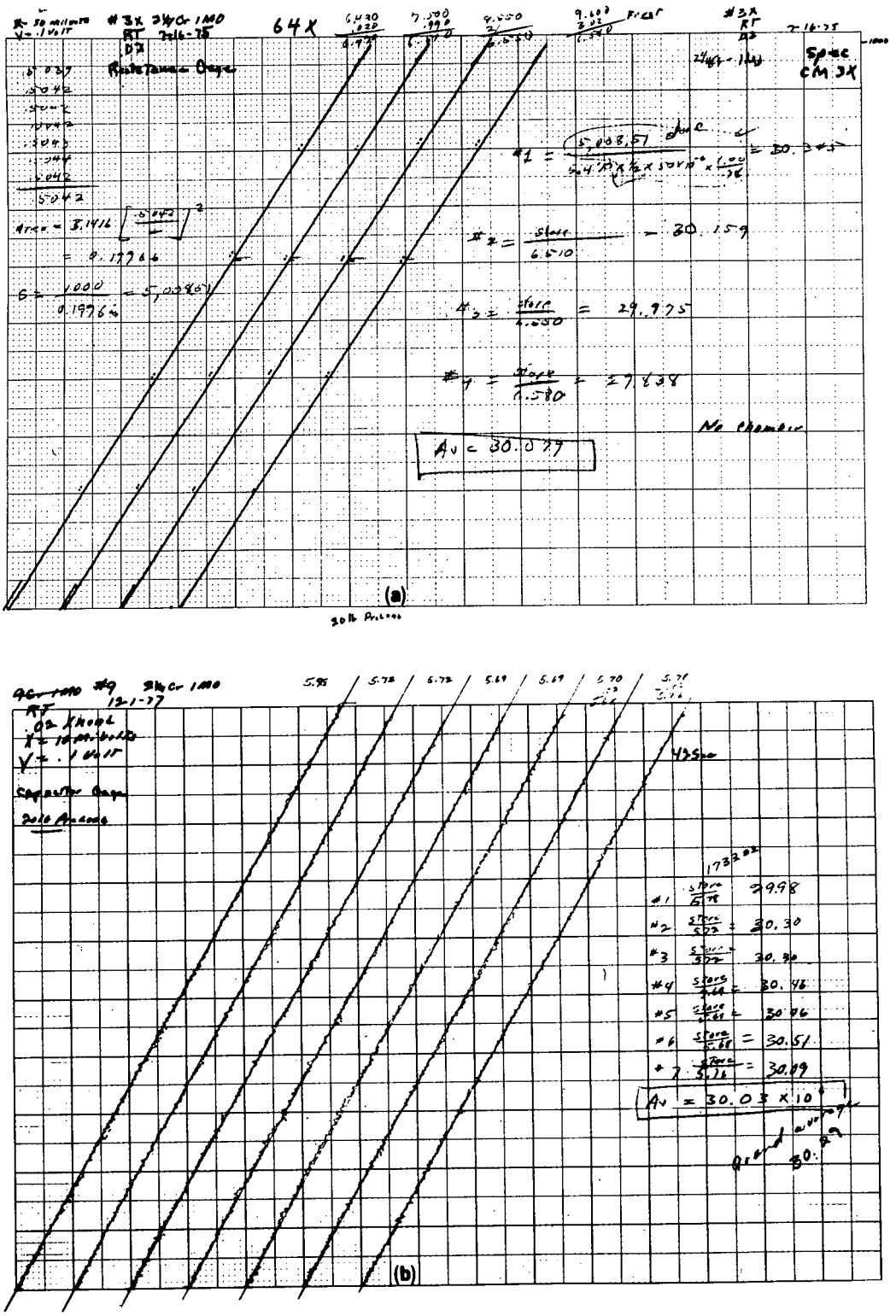

Fig. 9. Comparison of Stress-Strain Graphs Produced by the Weldable Resistance (a) and Capacitive (b) Gages.

Table 4. Coefficients of Polynomial Models of Elastic Constants[a]

Materials and Constants		Coefficients of $X = X_0[1 + A(T - T_0) + B(T - T_0)^2 + C(T - T_0)^3]$				Standard Deviation of Fit to Equation
		X_0	A	B	C	
			Dynamic			
2 1/4 Cr-1 Mo						
E	GPa	214.48 ± 0.161	-3.05032×10^{-4}	-6.22360×10^{-9}	-1.71081×10^{-10}	0.474
	10^6 psi	31.108 ± 0.0234				0.0687
G	GPa	83.661 ± 0.0738	-2.09753×10^{-4}	-4.53940×10^{-7}	2.72752×10^{-10}	0.645
	10^6 psi	12.134 ± 0.0107				0.0935
ν		0.28187 ± 0.000287	-4.66649×10^{-4}	2.19339×10^{-6}	-2.13668×10^{-9}	0.000279
304 Stainless Steel						
E	GPa	200.06 ± 0.324	-4.41980×10^{-4}	3.07524×10^{-9}	4.02024×10^{-11}	0.352
	10^6 psi	29.016 ± 0.0470				0.0510
G	GPa	77.511 ± 0.128	-5.11971×10^{-4}	1.40744×10^{-7}	-7.00466×10^{-11}	0.330
	10^6 psi	11.242 ± 0.0185				0.0478
ν		0.29049 ± 0.000544	3.54637×10^{-4}	-7.07393×10^{-7}	6.59136×10^{-10}	0.000313
316 Stainless Steel						
E	GPa	198.00 ± 0.848	-3.93625×10^{-4}	-8.37648×10^{-8}	9.26214×10^{-11}	0.639
	10^6 psi	28.718 ± 0.123				0.0927
G	GPa	76.739 ± 0.161	-4.72563×10^{-4}	-4.05496×10^{-9}	5.80860×10^{-11}	0.569
	10^6 psi	11.130 ± 0.0234				0.0825
ν		0.29015 ± 0.00113	3.55518×10^{-4}	-2.20321×10^{-7}	1.18177×10^{-10}	0.0000493
Incoloy 800H						
E	GPa	194.21 ± 1.365	-3.64822×10^{-4}	7.06294×10^{-8}	-6.53397×10^{-11}	0.655
	10^6 psi	28.168 ± 0.198				0.0950
G	GPa	74.877 ± 0.549	-2.50350×10^{-4}	-4.31878×10^{-7}	3.39907×10^{-10}	0.623
	10^6 psi	10.860 ± 0.0798				0.0904
ν		0.29692 ± 0.00219	-6.05000×10^{-4}	2.66177×10^{-6}	2.10991×10^{-9}	0.00116
			Static			
2 1/4 Cr-1 Mo						
E (LVDT)	GPa	207.46 ± 1.227	-1.02961×10^{-4}	-7.20162×10^{-8}	-5.73224×10^{-11}	0.0310
	10^6 psi	30.090 ± 0.178				0.00450
E (capacitance)	GPa	209.80 ± 1.482	-1.28266×10^{-4}	-4.58089×10^{-8}	-6.55302×10^{-11}	0.00696
	10^6 psi	30.429 ± 0.215				0.00101
G (capacitance)	GPa	81.996	-1.16229×10^{-4}	-9.93115×10^{-8}	-4.88666×10^{-11}	0.0069
	10^6 psi	11.892				0.0010
ν (capacitance)		0.28187 ±0.000287	6.05627×10^{-4}	-1.32036×10^{-7}	2.02259×10^{-10}	0.00148
304 Stainless Steel						
E (LVDT)	GPa	196.27 ± 1.528	-2.38802×10^{-4}	-1.10056×10^{-8}	2.37683×10^{-12}	0.00765
	10^6 psi	28.466 ± 0.222				0.00111

[a]Where temperature is expressed in °C. T_0 = 24°C (75°F).

Table 5. Dynamic Elastic Constants of 2 1/4 Cr-1 Mo Steel

Temperature		Young's Modulus		Shear Modulus		Poisson's Ratio
(°C)	(°F)	(GPa)	(psi)	(GPa)	(psi)	
24	75	214.5	31.11×10^6	83.7	12.13×10^6	0.282
38	100	213.7	30.99	83.4	12.10	0.280
66	150	211.8	30.72	82.9	12.02	0.278
93	200	210.0	30.46	82.3	11.94	0.275
121	250	208.2	30.19	81.6	11.84	0.275
149	300	206.3	29.92	80.9	11.74	0.274
177	350	203.8	29.65	80.2	11.63	0.274
204	400	202.5	29.37	79.4	11.52	0.275
232	450	200.6	29.09	78.6	11.40	0.276
260	500	198.6	28.80	77.7	11.27	0.277
288	550	196.5	28.50	76.8	11.14	0.279
316	600	194.4	28.20	75.9	11.01	0.281
343	650	192.4	27.93	74.9	10.87	0.283
371	700	190.2	27.58	74.0	10.73	0.285
399	750	188.0	27.26	73.0	10.59	0.287
427	800	185.6	26.92	72.0	10.44	0.290
454	850	183.2	26.58	70.9	10.29	0.292
482	900	180.8	26.22	69.9	10.14	0.294
510	950	178.2	25.85	68.8	9.98	0.295
538	1000	175.6	25.47	67.8	9.83	0.296
566	1050	172.9	25.08	66.7	9.67	0.297
593	1100	170.2	24.68	65.6	9.52	0.297
621	1150	167.3	24.26	64.5	9.36	0.296
649	1200	164.2	23.82	63.5	9.21	0.294

Observe that the repeated use of a single specimen resulted in moderate lowering of the Young's modulus of these materials at the high temperatures (compare curves with circles), but in the temperature ranges generally prescribed for their use the effect is not very significant. For 2 1/4 Cr-1 Mo steel at 482°C (900°F) the "softening" was only 0.6%, and for type 304 stainless steel at 538°C (1000°F) it was only 0.9%.

Table 6. Static Elastic Constants of 2 1/4 Cr-1 Mo Steel Established with LVDT and Capacitative Gages

Temperature		Young's Modulus from LVDT Gages		Constants Established with Capacitative Gages				Poisson's Ratio
				Young's Modulus		Shear Modulus		
(°C)	(°F)	(GPa)	(psi)	(GPa)	(psi)	(Gpa)	(psi)	
24	75	207.5	30.09×10^6	209.8	30.43×10^6	81.8	11.87×10^6	0.282
38	100	206.9	30.01	209.1	30.33	81.7	11.85	0.282
66	150	205.8	29.84	207.7	30.13	81.2	11.78	0.283
93	200	204.5	29.67	206.3	29.92	80.7	11.70	0.284
121	250	203.2	29.47	204.7	29.69	80.0	11.61	0.284
149	300	201.8	29.26	203.1	29.46	79.4	11.51	0.285
177	350	200.2	29.04	201.4	29.21	78.7	11.41	0.285
204	400	198.5	28.79	199.6	28.95	77.9	11.30	0.285
232	450	196.7	28.53	197.6	28.66	77.0	11.17	0.286
260	500	194.8	28.25	195.6	28.37	76.3	11.04	0.287
288	550	192.7	27.94	193.4	28.05	75.2	10.90	0.288
316	600	190.4	27.62	191.0	27.71	74.1	10.75	0.289
343	650	188.0	27.26	188.5	27.35	73.0	10.59	0.290
371	700	185.4	26.89	185.9	26.96	71.8	10.42	0.292
399	750	182.6	26.48	183.0	26.55	70.6	10.24	0.294
427	800	179.6	26.05	180.0	26.11	69.3	10.05	0.296
454	850	176.4	25.58	176.8	25.64	67.8	9.84	0.299
482	900	173.0	25.09	173.3	25.14	66.3	9.62	0.303
510	950	169.4	24.56	169.7	24.61	64.7	9.39	0.302
538	1000	165.5	24.00	165.8	24.05	63.0	9.14	0.311
566	1050	161.4	23.41	161.7	23.45	61.2	8.88	0.316
593	1100	157.1	22.78	157.3	22.82	59.4	8.61	0.322
621	1150	152.5	22.11	152.7	22.15	57.4	8.32	0.328
649	1200	147.6	21.41	147.8	21.44	55.2	8.01	0.335
677	1250	142.4	20.66	142.6	20.64	53.0	7.69	0.343
704	1300	137.0	19.87	137.1	19.89	50.7	7.36	0.352
732	1350	131.3	19.04					

Table 7. Elastic Constants of Type 304 Stainless Steel (Heat 9T2796)

Dynamic Constants

Temperature		Young's Modulus		Shear Modulus		Poisson's Ratio	Static Young's Modulus From LVDT Gages	
(°C)	(°F)	(GPa)	(psi)	(GPa)	(psi)		(GPa)	(psi)
24	75	200.1	29.02×10^6	77.5	11.24×10^6	0.290	196.3	28.47×10^6
38	100	198.9	28.85	77.0	11.17	0.292	195.1	28.30
66	150	196.5	28.50	75.9	11.01	0.294	192.7	27.94
93	200	194.0	28.14	74.9	10.86	0.296	190.4	27.61
121	250	191.6	27.79	73.8	10.70	0.298	188.0	27.27
149	300	189.1	27.43	72.7	10.55	0.300	185.6	26.92
177	350	186.7	27.08	71.7	10.40	0.301	183.2	26.57
204	400	184.2	26.72	70.7	10.26	0.303	180.8	26.23
232	450	181.8	26.37	69.7	10.11	0.304	178.4	25.88
260	500	179.4	26.02	68.7	9.97	0.305	176.0	25.53
288	550	177.0	25.67	67.7	9.82	0.307	173.6	25.17
316	600	174.6	25.33	66.7	9.68	0.308	171.1	24.82
343	650	172.2	24.98	65.8	9.54	0.309	168.7	24.47
371	700	169.9	24.64	64.9	9.41	0.309	166.2	24.11
399	750	167.5	24.29	63.9	9.27	0.310	163.8	23.76
427	800	165.1	23.95	62.9	9.13	0.311	161.3	23.40
454	850	162.9	23.62	61.1	9.00	0.312	158.9	23.04
482	900	160.5	23.28	61.2	8.87	0.313	156.4	22.68
510	950	158.2	22.95	60.2	8.73	0.314	153.9	22.32
538	1000	156.0	22.62	59.3	8.60	0.315	151.4	21.96
566	1050	153.7	22.29	58.4	8.47	0.316	148.9	21.60
593	1100	151.5	21.97	57.5	8.34	0.318	146.5	21.24
621	1150	149.3	21.65	56.6	8.21	0.319	144.0	20.88
649	1200	147.1	21.33	55.7	8.08	0.321	141.5	20.52
677	1250	144.9	21.02	54.8	7.95	0.323	139.0	20.16
704	1300	142.8	20.71	53.8	7.81	0.325	136.5	19.79
732	1350	140.7	20.40	53.0	7.68	0.328	134.0	19.43
760	1400	138.6	20.10	52.1	7.55	0.331	131.5	19.07
788	1450	136.5	19.80	51.2	7.42	0.334	128.9	18.70
816	1500	134.5	19.51	50.3	7.29	0.338	126.4	18.34
843	1550	132.5	19.22	49.4	7.16	0.342	123.9	17.79
871	1600	130.6	18.94	48.5	7.03	0.347	121.4	17.61

Table 8. Dynamic Elastic Constants of Type 316 Stainless Steel

Temperature		Young's Modulus		Shear Modulus		Poisson's Ratio
(°C)	(°F)	(GPa)	(psi)	(GPa)	(psi)	
24	75	198.2	28.74×10^6	76.81	11.14×10^6	0.291
38	100	197.1	28.59	76.26	11.06	0.292
66	150	194.9	28.27	75.29	10.92	0.295
93	200	192.7	27.95	74.26	10.77	0.297
121	250	190.4	27.62	73.22	10.62	0.300
149	300	188.2	27.30	72.26	10.48	0.303
177	350	185.9	26.97	71.22	10.33	0.305
204	400	183.7	26.64	70.26	10.19	0.307
232	450	181.4	26.31	69.22	10.04	0.310
260	500	179.1	25.97	68.26	9.90	0.312
288	550	176.8	25.64	67.29	9.76	0.314
316	600	174.5	25.31	66.26	9.61	0.316
343	650	172.2	24.97	65.29	9.47	0.318
371	700	169.9	24.64	64.33	9.33	0.320
399	750	167.5	24.30	63.36	9.19	0.322
427	800	165.3	23.97	62.40	9.05	0.324
454	850	163.0	23.64	61.43	8.91	0.326
482	900	160.7	23.31	60.54	8.78	0.328
510	950	158.4	22.98	59.57	8.64	0.330
538	1000	156.2	22.66	58.67	8.51	0.332
566	1050	154.0	22.33	57.78	8.38	0.333
593	1100	151.8	22.01	56.81	8.24	0.335
621	1150	149.6	21.70	55.99	8.12	0.337
649	1200	147.4	21.38	55.09	7.99	0.339
677	1250	145.3	21.07	54.19	7.86	0.340
704	1300	143.2	20.77	53.57	7.74	0.342
732	1350	141.1	20.47	52.54	7.62	0.344
760	1400	139.1	20.17	51.71	7.50	0.346
788	1450	137.1	19.88	50.88	7.38	0.347
816	1500	135.1	19.60	50.06	7.26	0.349
843	1550	133.2	19.32	49.30	7.15	0.351
871	1600	131.3	19.05	48.54	7.04	0.353

Table 9. Dynamic Elastic Constants of Alloy 800H

Temperature		Young's Modulus		Shear Modulus		Poisson's Ratio
(°C)	(°F)	(GPa)	(psi)	(GPa)	(psi)	
24	75	194.3	28.18×10^6	74.88	10.86×10^6	0.297
38	100	193.3	28.04	74.60	10.82	0.295
66	150	191.3	27.75	74.05	10.74	0.292
93	200	189.4	27.47	73.43	10.65	0.290
121	250	187.6	27.20	72.81	10.56	0.288
149	300	185.6	26.92	72.12	10.46	0.287
177	350	183.7	26.65	71.36	10.35	0.287
204	400	181.9	26.38	70.60	10.24	0.288
232	450	180.0	26.11	69.84	10.13	0.289
260	500	178.2	25.84	69.02	10.01	0.291
288	550	176.3	25.57	68.19	9.89	0.293
316	600	174.6	25.31	67.29	9.76	0.296
343	650	172.6	25.04	66.47	9.64	0.299
371	700	170.8	24.77	65.57	9.51	0.303
399	750	169.0	24.51	64.67	9.38	0.306
427	800	167.1	24.24	63.78	9.25	0.310
454	850	165.3	23.98	62.88	9.12	0.315
482	900	163.5	23.71	61.98	8.99	0.319
510	950	161.6	23.44	61.09	8.86	0.323
538	1000	159.7	23.17	60.19	8.73	0.327
566	1050	157.9	22.90	59.29	8.60	0.331
593	1100	156.0	22.63	58.47	8.48	0.335
621	1150	154.2	22.36	57.57	8.35	0.338
649	1200	152.2	22.08	56.74	8.23	0.341
677	1250	150.4	21.81	55.99	8.12	0.343
704	1300	148.4	21.53	55.23	8.01	0.345
732	1350	146.4	21.24	54.47	7.90	0.345
760	1400	144.5	20.96	53.71	7.79	0.345
788	1450	142.5	20.67	53.09	7.70	0.343
816	1500	140.5	20.38	52.40	7.60	0.340
843	1550	138.4	20.08	51.85	7.52	0.336
871	1600	136.4	19.78	51.30	7.44	0.330
899	1650	134.3	19.48	50.81	7.37	0.322

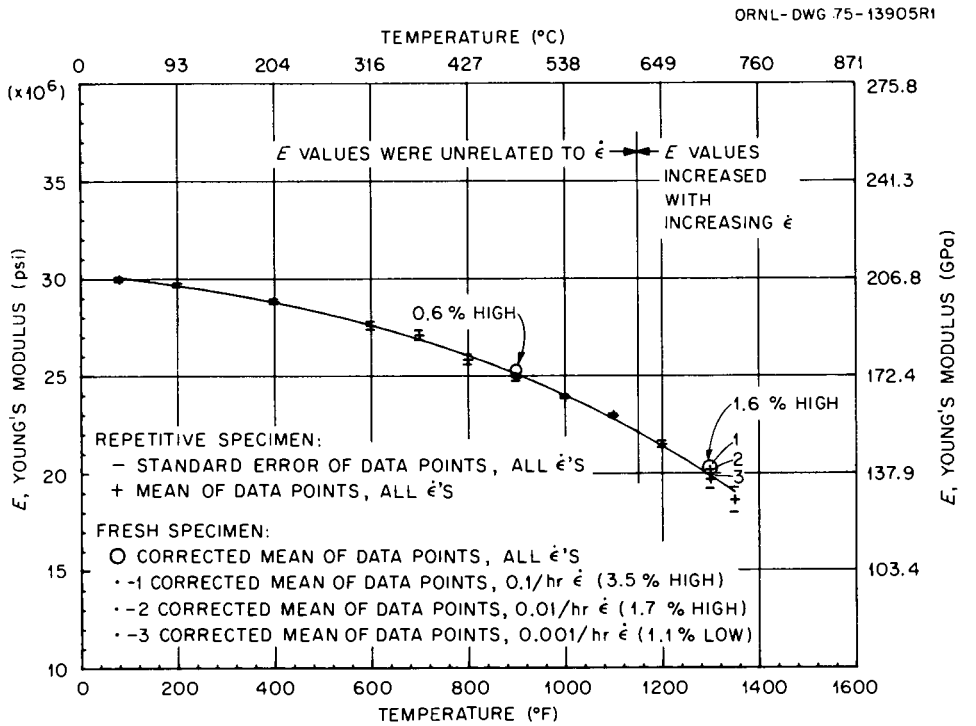

Fig. 10. Static Young's Modulus of 2 1/4 Cr–1 Mo Steel Determined with LVDT Gages.

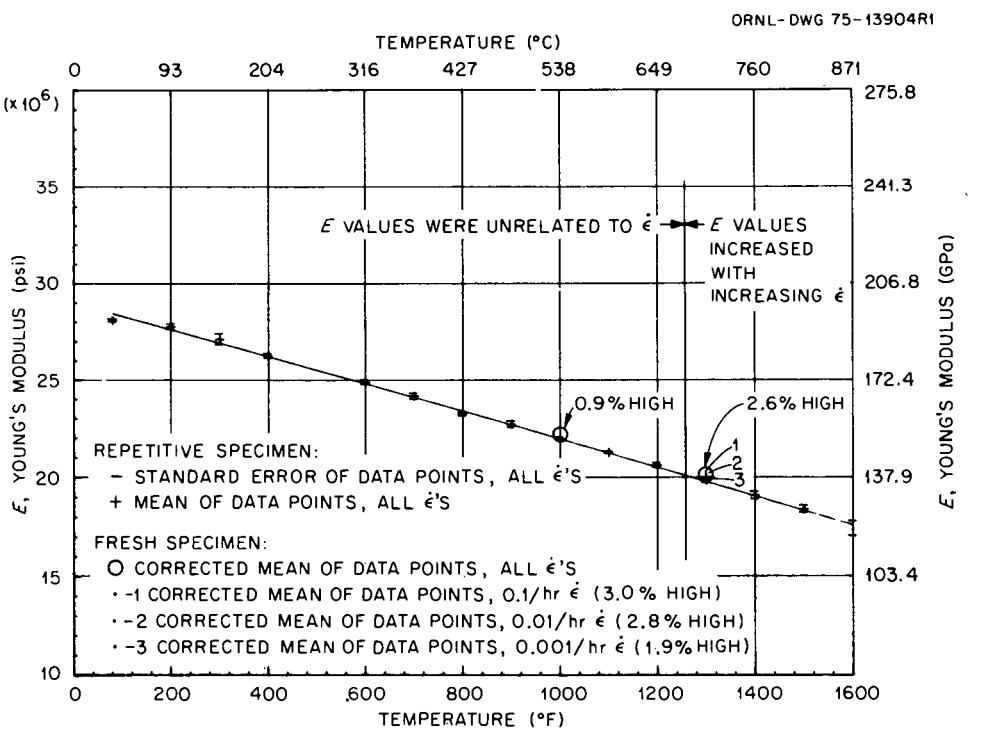

Fig. 11. Static Young's Modulus of Type 304 Stainless Steel (Heat 9T2796) Determined with LVDT Gages.

Strain rate apparently had a small effect on E values of 2 1/4 Cr-1 Mo steel at 649°C and higher (Fig. 10) and a 704°C and higher in type 304 stainless steel (Fig. 11). The curve for 2 1/4 Cr-1 Mo steel tends to turn downward with temperature, while the type 304 curve is nearly straight.

After test schedules were qualified for determining elastic constants as a function of temperature by the reference LVDT method, the same procedures were used in static tests with other gages.

2 1/4 Cr-1 Mo Steel

The dynamic models of E, G, and ν for 2 1/4 Cr-1 Mo steel are shown in Fig. 12, whereas the static curves of E, G, and ν for 2 1/4 Cr-1 Mo steel measured with the capacitive gages are given in Fig. 13. Observe in Fig. 12 that E and G data points rather closely fit the curves, as is confirmed by the standard deviations of fit in Table 4. This reasonably good fit of data to the models is characteristic of the dynamic method.

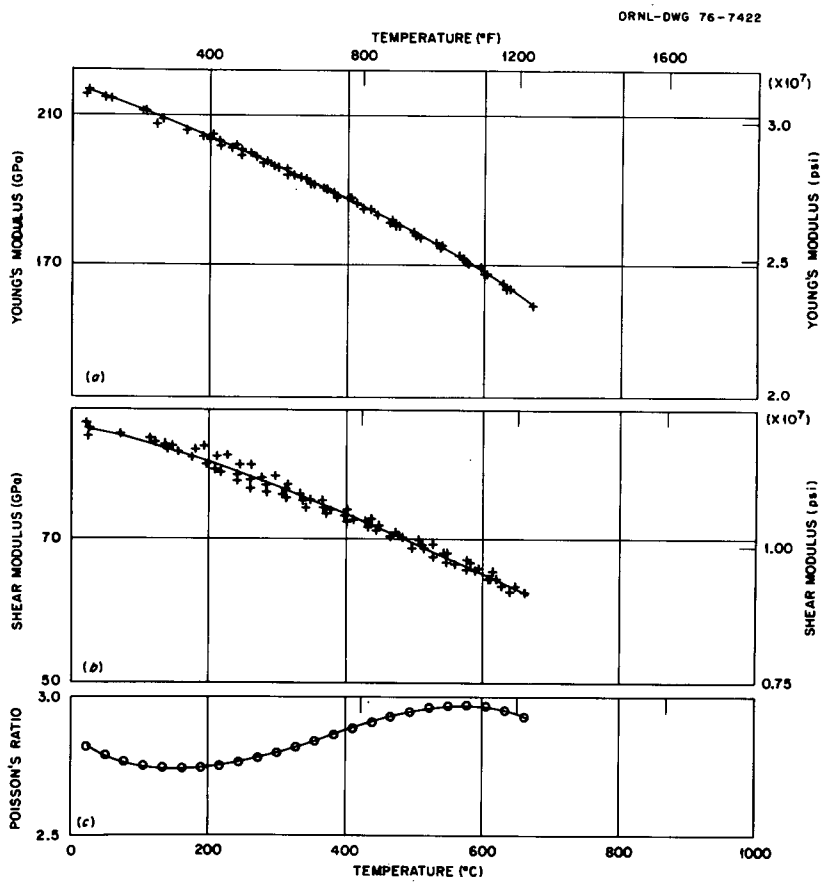

Fig. 12. Dynamic Elastic Constants of 2 1/4 Cr-1 Mo Steel.

The ν data, on the other hand, are seen to exactly fit the Poisson's ratio curve. However, this is because dynamic ν was derived from *E* and *G* by the basic relationship equating these constants [Eq. (2)]. This is deceiving since, as will be shown subsequently, the dynamic ν models are not as consistent as the *E* and *G* ones.

The good degree of fit of the *E* and ν data points to the static models in Fig. 13 is shown by the standard error limits included in these graphs. Here the *G* data conform exactly with the shear modulus curve because in the static case *G* was derived from *E* and ν [Eq. (3)].

Figure 14 compares our dynamic *E* curve for 2 1/4 Cr-1 Mo steel with the static *E* curves established with LVDT and capacitive gages. The ASME Code values of static *E* are included for comparison.

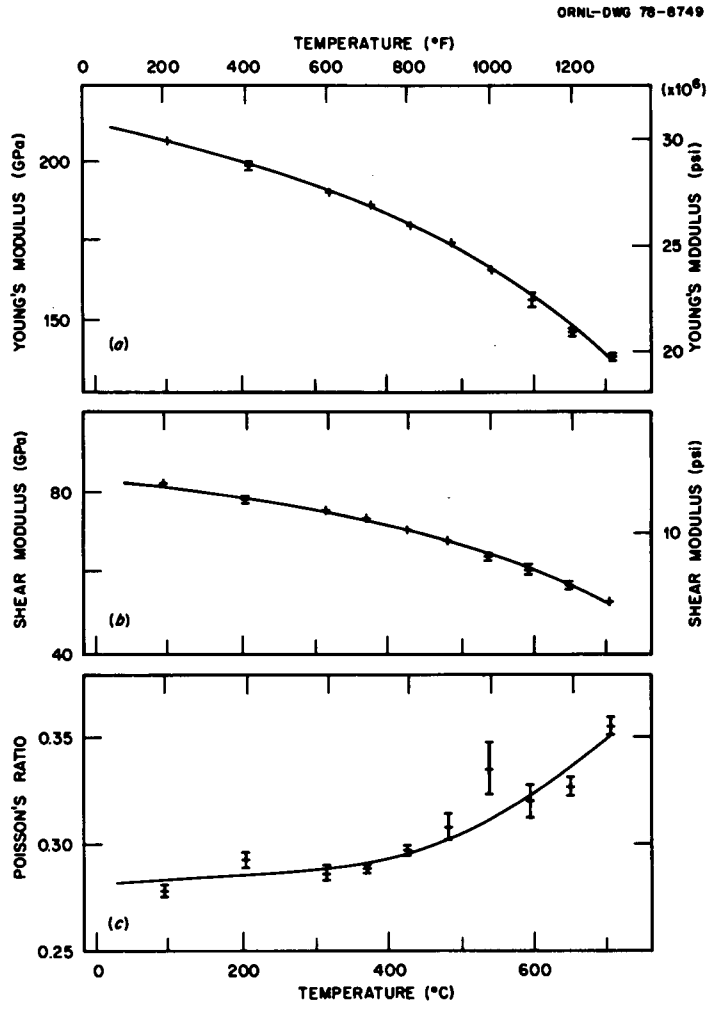

Fig. 13. Static Elastic Constants of 2 1/4 Cr-1 Mo Steel Determined with Capacitive Gages.

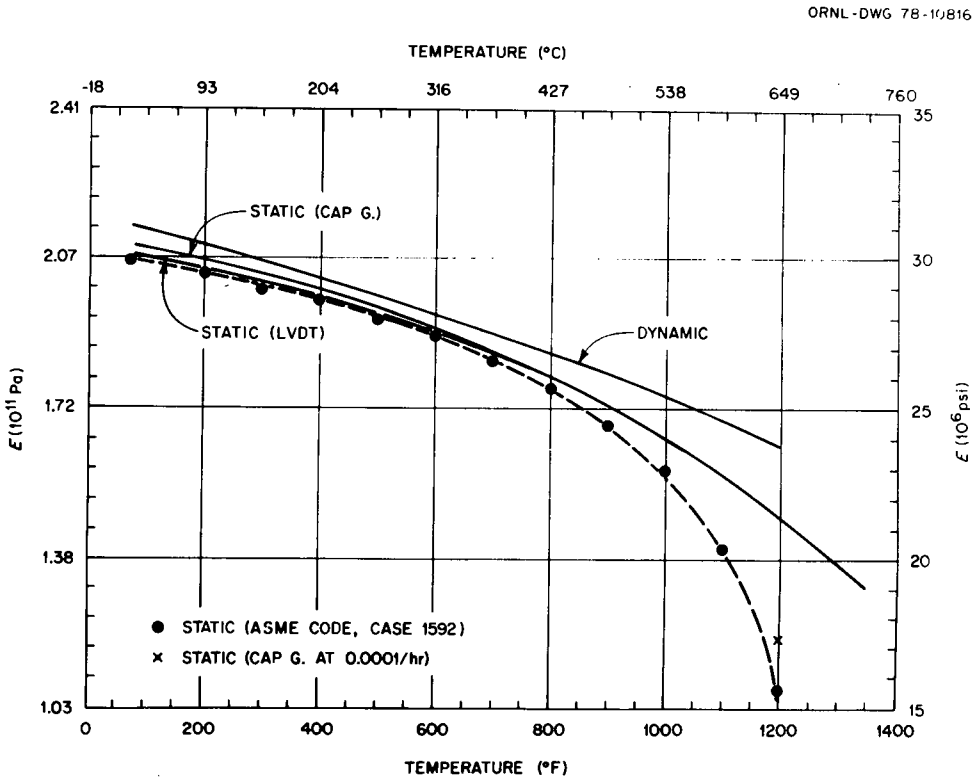

Fig. 14. Comparison of Young's Modulus Curves of 2 1/4 Cr–1 Mo Steel.

It is noteworthy that the dynamic curve lies above the static curves and that the static curve determined with the capacitive gages nearly coincides with that established by our reference LVDT method. At the higher temperatures they superimpose. The code curve conforms to the other static curves at temperatures up to about 371°C (700°F), where it begins to rapidly drop off. At 649°C (1200°F) it is approximately 27% lower than the other static E curves.

Whereas our static E curves were determined by combining measurements made at strain rates of 0.01 and 0.001/h (strained to 100×10^{-6}) for the capacitive curve, additional tests were made with the capacitive gages at 649°C at one decade still lower strain rate (actually 0.000087/h) to examine the effect of very low strain rate. The average of two tests, which took about 1.2 h per test, gave an E value of 119.6 GPa (17.35×10^6 psi). This approximates the code value at this temperature (Fig. 14), and there would appear to be little doubt that these low code values of E were influenced by creep.

The dynamic and static Poisson's ratio curves of 2 1/4 Cr-1 Mo steel (Figs. 12 and 13) are compared in Fig. 15. The static ν data of Garofalo,[14] which he derived from *E* and *G*, are included with our model of his data. Our dynamic and static Poisson's ratio curves lie relatively close together up to about 427°C (800°F), where the static curve rises while the dynamic one levels off. Because our static ν curve was determined directly with capacitive gages whereas the dynamic curve and Garofalo's static curve were derived from *E* and *G* data, it should be subject to less error than the other two and is preferred.

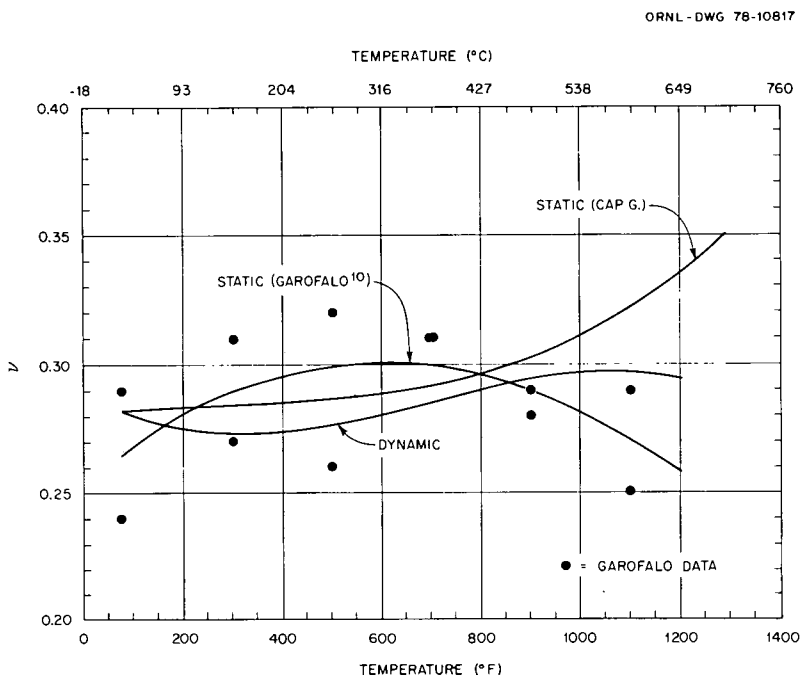

Fig. 15. Comparison of Poisson's Ratio Curves of 2 1/4 Cr-1 Mo Steel.

Type 304 Stainless Steel

The dynamic elastic constant curves of the type 304 stainless steel (heat 9T2796) with data points superimposed are presented in Fig. 16. Both *E* and *G* decrease approximately linearly with temperature, whereas ν shows a slight sinusoidal effect before curving upward at high temperature.

---

[14]F. Garofalo, P. R. Malenock, and G. V. Smith, "The Influence of Temperature on the Elastic Constants of Some Commercial Steels," pp. 10–30 in *Symposium on Determination of Elastic Constants, ASTM Spec. Tech. Publ.* 129, American Society for Testing and Materials, Philadelphia, 1952.

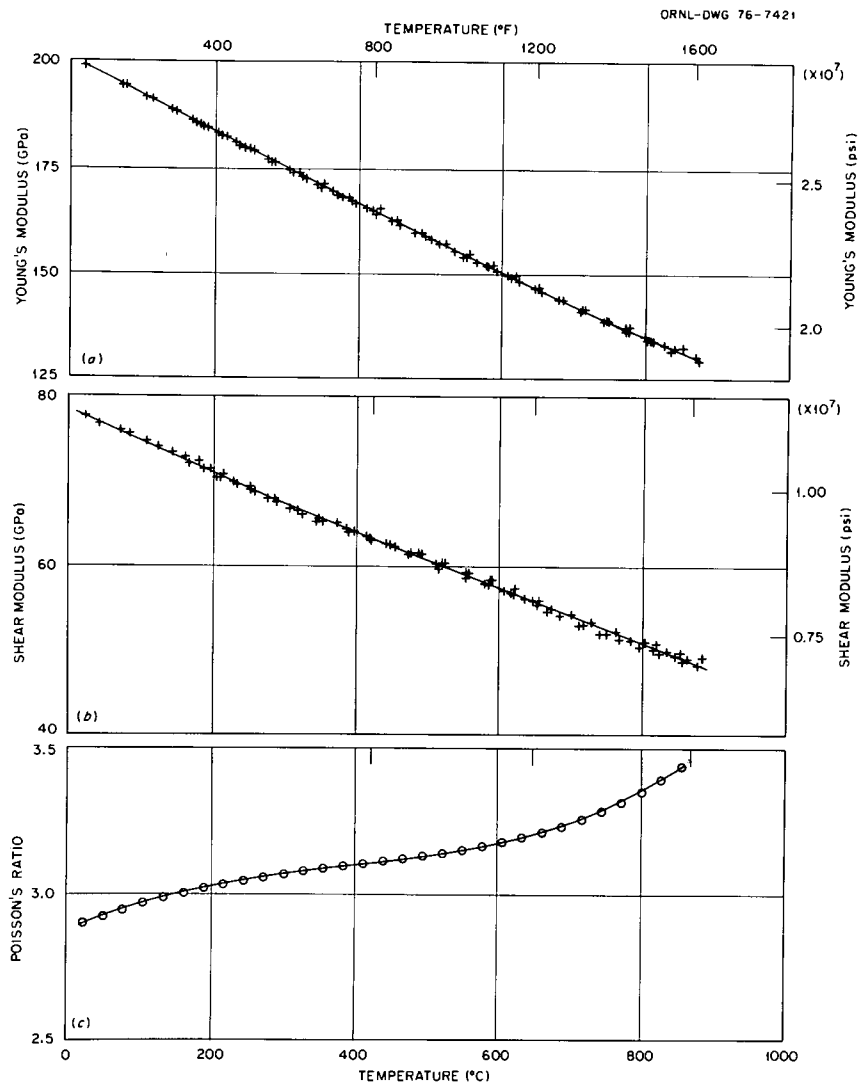

Fig. 16. Dynamic Elastic Constants of Type 304 Stainless Steel, Heat 9T2796.

The dynamic Young's modulus curve (Fig. 16) and the static E curve (Fig. 11) with ASME Code values superimposed are compared in Fig. 17. The static curve again lies below the dynamic one and is approximately parallel to it. At room temperature the static E is about 3% lower than the dynamic E. The static code values conform to our static values at the temperature extremes but more closely approximate the dynamic curve at the intermediate temperatures.

The influence of heat-to-heat variations on the dynamic elastic constant curves of type 304 stainless steel was determined. The effects are illustrated in Fig. 18, which contains three heats of type 304 stainless steel along with curves for the other alloy types we examined.

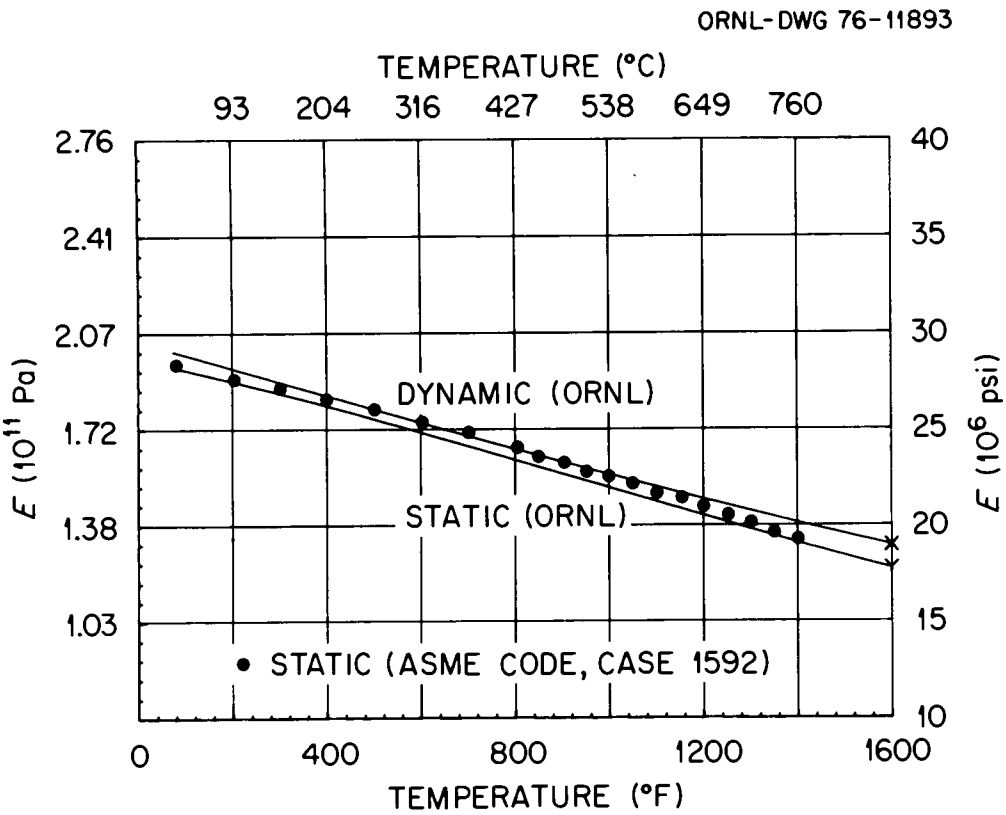

Fig. 17. Comparison of Young's Modulus Curves of Type 304 Stainless Steel, Heat 9T2796.

These curves were constructed from the computed dynamic elastic constants[15] of Tables 5, 6, 8, and 9.

Observe that the dynamic E and G values of type 304 stainless steel vary very little between heats, whereas the curves for ν are distinctly different. Because the variations in E and G are so small, the curves of heat 9T2796 (dashed) only are shown. However, curves of ν are shown for all three heats of type 304 stainless steel since ν varied considerably between heats.

The large difference seen in the Poisson's ratio curves of the three heats of type 304 stainless steel no doubt result from the fact that the ν data are derived and the effects displayed are not believed to be real.

---

[15]Computed elastic constants of heats 60551 and 346544 of type 304 stainless steel were obtained from M. W. Moyer and T. W. Dews, *Summary of Accoustic Properties of Several LMFBR and HTGR Materials*, Y-DA-6651 (February 1976).

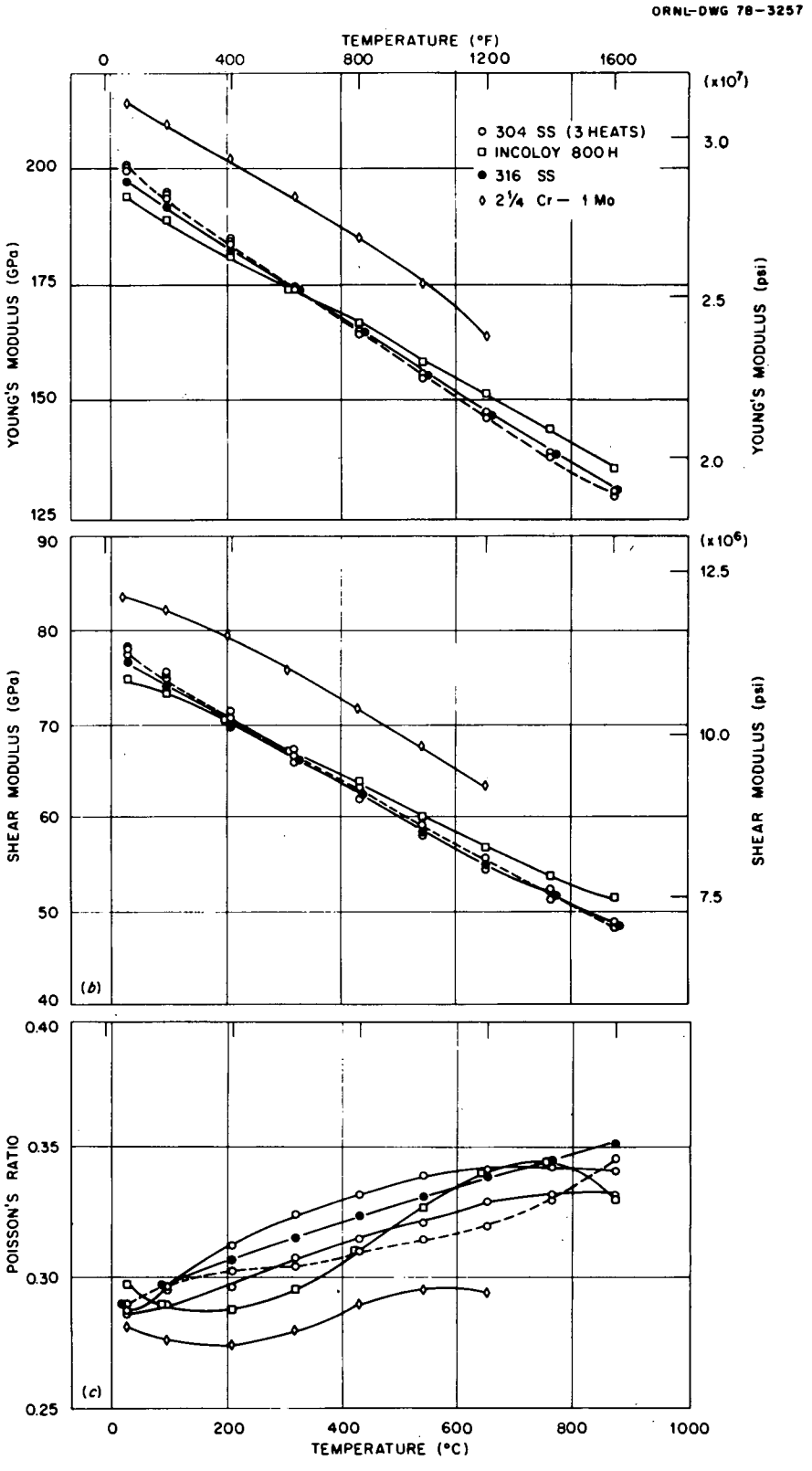

Fig. 18. Comparisons of the Dynamic Elastic Constants Curves of the Various Alloys.

The decidedly different curve shapes probably result from errors in E and G in one instance reinforcing in one direction, in another reinforcing in the other direction, and in still another case canceling.

Type 316 Stainless Steel

The dynamic modulus curves of type 316 stainless steel are shown in Fig. 19. The E and G curves are quite similar to those for type

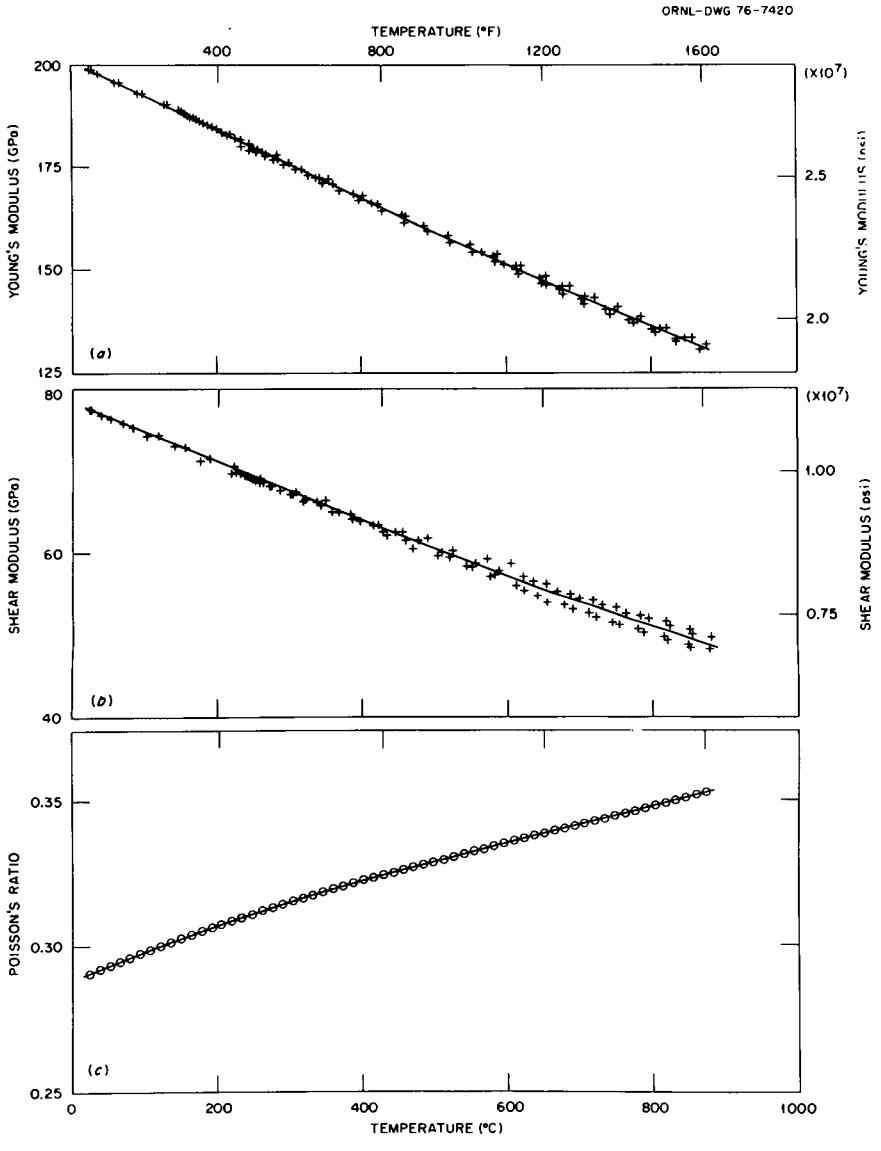

Fig. 19. Dynamic Elastic Constants of Type 316 Stainless Steel.

304 stainless steel (Fig. 16). The Young's modulus for type 316 stainless steel at room temperature is slightly below those for type 304 (Fig. 18). At elevated temperature resolution is not as good and any difference between it and the type 304 stainless steels may not be significant.

Alloy 800H

The dynamic modulus curves of alloy 800H are presented in Fig. 20. Again, E and G decrease approximately linearly with temperature. Here the ν curve shows an exaggerated sinusoidal characteristic, as contrasted

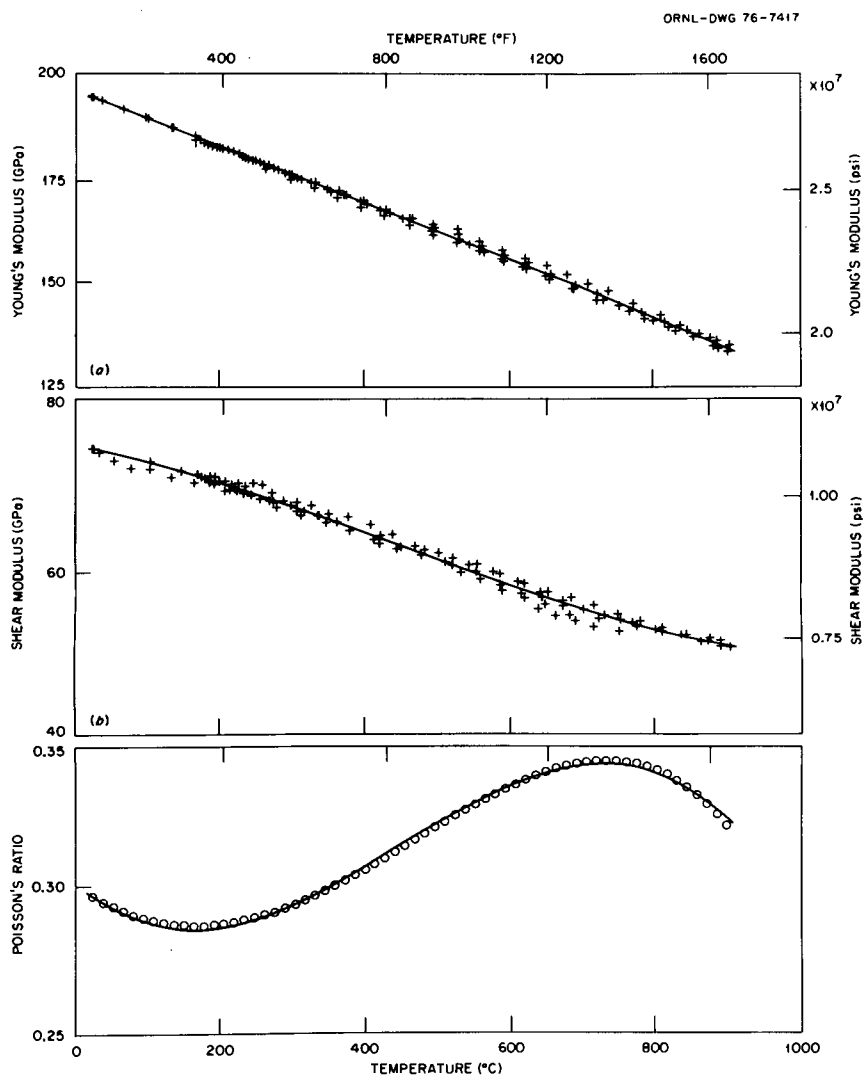

Fig. 20. Dynamic Elastic Constants of Alloy 800H.

to the nearly linear ν curve for the preceeding type 316 stainless steel (Fig. 19). Again, however, this effect probably is not real. Significantly, the dynamic values of E and G of alloy 800H at room temperature lie somewhat below those for the stainless steels (Fig. 18). At an intermediate temperature they cross over, and at 400°C and higher they are considerably higher than those of the stainless steels.

It will be noted in Fig. 18 that the E and G values of the various alloys appear to be somewhat related, and the trends for one constant seem to hold for the other. For the types 304 and 316 stainless steels and alloy 800H (materials of face-centered cubic crystal structure), the E and G values do not vary by more than about 3.5% at room temperature nor by more than about 5.5% at the highest temperature. On the other hand, the body-centered cubic 2 1/4 Cr-1 Mo steel is substantially higher in both Young's modulus and shear modulus at all temperatures than any of the face-centered cubic materials.

DISCUSSION OF RESULTS

The dynamic method of determining elastic constants is basically a more economical and timesaving process than the static method. Moreover, the amount of material required for test generally is less, and basically it is nondestructive. As a consequence, this method has enjoyed wide use. However, whereas static elastic constants are established under conditions directly relatable to engineering applications, the relevance of dynamic constants is less clear. This is because they are derived from the velocity of sound waves within the solid instead of from macroscopic strain imposed by external load. One means of assessing the relevance of dynamic elastic constants is to compare them on a broad basis with static constants measured under controlled test conditions, as we have begun to do here.

The fact that we obtained equivalent Young's modulus curves for 2 1/4 Cr-1 Mo steel by two separate static methods of test (with the LVDT and the capacitive gages), which in turn were confirmed by the ASME Code values (at lower temperatures), suggests that our reference static test method employing LVDT gages gives reasonably accurate

results. Clearly the method employing capacitive gages gives equally good E data and has potential for accurately measuring ν and G by deduction.

It is significant that the dynamic Young's modulus models for both 2 1/4 Cr-1 Mo steel and type 304 stainless steel were approximately parallel to the static models and at room temperature were only about 3% higher. In separate similar elastic studies[16] on face-centered cubic Inconel 718, the relationship between the dynamic and static curves was very similar to that presented here for type 304 stainless steel. That is, the models again were approximately parallel, and at room temperature the dynamic E value was about 3% higher than the static.

That our dynamic Young's moduli ran somewhat higher than the static moduli is not an uncommon observation and, indeed, some[17,18] have used thermodynamic considerations to explain their difference. The slow or static loading method is said to give isothermal (constant-temperature) elastic constants, whereas the rapid or dynamic method gives adiabetic (constant-entropy) constants. For most engineering materials this distinction should result in a difference of about 1% in Young's modulus.[18] This distinction in the dynamic and static processes, however, is not considered to hold for the shear modulus. Isothermal and aidabetic shear moduli should be equivalent since shear at constant volume and entropy leaves temperature unaffected.[18]

A second reason for the dynamic moduli being higher than the static may reside in the large difference in magnitudes of strain involved in the two test methods. Whereas strain by the static method is of macro proportions, in the sonic transmission technique atoms are barely moved from their equilibrium sites. This distinction would appear to have a

---

[16] J. P. Hammond, D. Donsback, and C. R. Brinkman, *Elastic Constants of Inconel 718*, report in preparation.

[17] E. Schreiber et al., *Elastic Constants and Their Measurement*, McGraw-Hill, New York, 1973.

[18] R. P. Reed, "Elastic Properties of Metal and Alloys in Iron, Nickel, and Iron-Nickel Alloys," *J. Phys. Chem. Ref. Data* 2(3): 531-617 (1973).

bearing since the first derivative of force with respect to atomic displacement, which is an expression of Young's modulus, is seen to decrease as the atoms of the lattice are separated.[19] Thus, Young's modulus should be somewhat lower for the static method, where the mean atomic displacement is large in comparison with that of the dynamic case.

In viewing the foregoing considerations together with the elastic constant results obtained here, a practical application of the dynamic data could well include a downward adjustment of the dynamic moduli to bring them in line with the static. For dynamic E an adjustment at all temperatures amounting to about 3% of the static value at room temperature would seem appropriate. The dynamic G values could be diminished similarly to a smaller extent or not at all.

Because the dynamic Poisson's ratio is derived and will be in error to the extent that errors in E and G reinforce or balance out, the dynamic ν data should be used cautiously. The room-temperature dynamic ν data were determined by a more accurate means than that at elevated temperature and thus are more reliable. Dynamic ν at room temperature may not require an adjustment.

The method of test using capacitive gages in conjunction with the "repetitive" specimen technique shows much promise and should provide a needed means for establishing good E and ν data under specific use conditions. A constructive modification of the capacitive gage would be to stiffen its attachment ribbons while at the same time reducing the stiffness of the sensor flexture that mounts above the capacitor plates for maintaining their concentricity. This change would facilitate more efficient transfer of specimen strain to the gage.

The measurements made of the anisotropy index of the various test specimens revealed that isotropy varied substantially. The results of these measurements are given in Table 10 along with the dynamic E value of the specimen and the dimensions and condition of the product form from which it was taken.

---

[19]L. H. Van Vlack, *Elements of Materials Science*, 2nd ed., Addison-Wesley, Reading, Mass., April 1967.

Table 10. Anisotropy Indices[a] of Test Specimens

Alloy	Heat	Form	Dimension (mm)	Dimension (in.)	Specimen Condition	E (GPa)	Anisotropy Index (m/s)
2 1/4 Cr-1 Mo	20017	Plate	25	1	IA	214.5	0.073
Type 304 stainless steel	9T2976	Plate	25	1	SA	200.1	41.731
Type 304 stainless steel	346544	Plate	51	2	SA	201.2	1.248
Type 304 stainless steel	60551	Bar	127 × 178	5 × 7	SA	200.3	0.132
Type 316 stainless steel	8092297	Plate	25	1	SA	198.0	0.304
Alloy 800H	HHG758A	Plate	30	1.2	SA	194.2	43.604

Notes: Test specimens were taken with their axes parallel to the rolling direction from central locations. E = Young's modulus; IA = isothermally annealed (see Table 1); SA = solution annealed.

[a]Index = $(V_{G_0} - V_{G_{90}})/2$ [Eq. (A23)].

Note that isotropy of the specimens in type 304 stainless steel improved (index reduced) greatly as the product form increased in size. The factor having greatest bearing on the anisotropy index of the alloys doubtlessly was the degree of preferredness of grain orientation. The anisotropy index in the specimens of type 304 stainless steel no doubt improved with product form size because the degree of preferred grain orientation diminished. This occurred as a result of less metalworking and annealing being required to process the material down to size. This consideration has led us to use larger product forms in the more recent elastic work.[16]

Whereas elastic constants of polycrystalline alloys ordinarily are influenced significantly by the crystallographic preferredness of grain structure,[20] in this particular instance of the series of type 304 stainless steel, the dynamic E values (RT) varied by only 0.5% (Table 10), which is nearly within the experimental error of the test method. The probable cause of this is that the specific crystallographic textures involved, though moderately different between specimens, were such as to fortuitously give nearly equal E values in the rolling direction of the plate or bar.[21]

---

[20]C. S. Barrett, *Structure of Metals*, McGraw-Hill, New York, 1952.

[21]J. P. Hammond, "Elastic Properties of Engineering Construction Materials," *Mechanical Properties Test Data for Structural Materials Quart. Prog. Rep. July 31, 1976*, ORNL-5200, pp. 129-41.

Interestingly, the 2 1/4 Cr-1 Mo steel specimen (Table 10) gave the lowest anisotropy index of all the specimens examined, although the material had been substantially reduced in forming the product form (25-mm plate). This high degree of isotropy, in spite of the large amount of metalworking, was attributed to a randomization of grain orientation that occurred with the metalworking and heat-treating of this material.[21] This randomization phenomenon is not uncommon with certain allotropic ferrous materials and, indeed, vendors frequently exploit it to improve the quality of their products.

The specimen of alloy 800H gave a very high anisotropy index, rivaling that of heat 9T2796 of type 304 stainless steel, which again is attributable to preferredness of grain orientation. That the specimen of type 316 stainless steel showed a comparatively low index in spite of having been processed to a relatively low thickness (25 mm) is somewhat surprising but doubtlessly is associated with a metalworking history that resulted in a comparatively low degree of preferred grain orientation.

SUMMARY AND CONCLUSIONS

The dynamic and static elastic constants (E, G, and ν) of 2 1/4 Cr-1 Mo steel, types 304 and 316 stainless steel, and alloy 800H were determined from room temperature to 649°C (1200°F) and higher. These data were treated and recorded as cubic polynomials for computing expected values of the constants as a function of temperature. The polynomial model used has three coefficients and is fitted to the total data by a least squares optimization of the coefficients. The model also contains the room-temperature value of the elastic constant and, further, has the property of intersecting it. Thus, accuracy is imparted to the model to the extent that this constant is accurately determined. For this reason the room-temperature elastic constants generally were established by more painstaking procedures.

The dynamic elastic constants were determined by a hybrid sonic method that incorporates a double-pulse, block-sample method for establishing room-temperature moduli and a single-pulse, thin-wire

method that uses a magnetostrictive transducer for gathering elevated-temperature data. This hybrid method gave room-temperature E, G, and ν values to a precision of 0.1 to 0.4% and modulus-temperature curves in E and G that were highly reproducible. However, because the dynamic ν was derived from values of E and G, the upper temperature regions of curves in it suffered inconsistencies. This resulted from small errors in E and G being reinforcing in such regions of the ν curves.

Three different methods distinguished by the strain transducers employed were evaluated for determining the static elastic constants at room and elevated temperatures. The transducers examined included (1) the type 6233 LVDT gage, (2) the weldable MG-425 resistance strain gage, and (3) the HTC-DC-100 capacitive strain gage. Because the LVDT method gave excellent results and its gages were nonexpendable and readily calibratable, it was used as a reference technique. However, this method was useful only for measuring E. The resistance strain gage method did not show adequate potential for obtaining good elastic constants values at high temperatures. The capacitive gage method gave excellent E data and showed high potential for obtaining good ν and G values to 816°C (1500°F). A novel "repititive" specimen technique was developed and used in conjunction with the three static test methods to improve their resolution at elevated temperatures. It foregoes the requirement of a separate test specimen for each data point. Corrections were made for the minor thermal-mechanical effects that stemmed from repeated use of the test specimen.

In the two materials for which both static and dynamic moduli were determined, 2 1/4 Cr-1 Mo steel and type 304 stainless steel, the dynamic Young's moduli generally ran higher than the static values (about 3% higher at room temperature). Theoretical reasons for this occurring were cited, and possible adjustments to the dynamic data enabling their more judicious use were discussed.

The static elastic constant test methods employing the reference LVDT gage and the capacitive gage gave Young's modulus curves for 2 1/4 Cr-1 Mo steel in very close agreement. These curves coincided with ASME Code (static) values for this material from room temperature to 371°C (700°F). However, above this temperature the Code values

dropped off rapidly and at 649°C (1200°F) were approximately 27% lower than our static values. This difference in static E was shown to be a function of the strain rate used in measuring the modulus, and it is likely that the low Code values are influenced by creep.

The Code (static) values of Young's modulus of type 304 stainless steel were compared with our dynamic and static E curves. They agreed with our static results at the curve extremes but fell closer to the dynamic curve at the intermediate temperatures.

Expected values E, G, and ν for the various materials studied were computed with the polynomials and are recorded at room temperature and at 28°C (50°F) intervals from 38 to 649°C (100 to 1200°F) and higher.

ACKNOWLEDGMENTS

The authors gratefully acknowledge Robin Williams and V. K. Sikka for criticizing the manuscript and P. Patriarca and G. M. Slaughter for reviewing the report. Also we acknowledge T. W. Dews for help in measuring dynamic constants. Our appreciation is extended to Sigfred Peterson for editing and to Graphic Arts for preparing the illustrations.

APPENDIX A

CALCULATIONS OF DYNAMIC ELASTIC CONSTANTS

Following are listed the equations necessary to calculate all the moduli and Poisson's ratios for a bulk sample knowing the longitudinal V_E and shear V_L velocities, and the density:

$$\nu = \frac{1 - 2(V_G/V_L)^2}{2 - 2(V_G/V_L)^2} , \tag{A1}$$

$$V_E = V_L\sqrt{\frac{(1 + \nu)(1 - 2\nu)}{1 - \nu}} , \tag{A2}$$

$$E = V_L^2\rho\frac{(1 + \nu)(1 - 2\nu)}{1 - \nu} , \tag{A3}$$

$$G = V_G^2\rho \text{ , and} \tag{A4}$$

$$K = \frac{E}{3(1 - 2\nu)} . \tag{A5}$$

Also, it is necessary to calculate an estimate of the standard deviation of each variable. An estimate of the standard deviation of a function of more than one variable can be obtained by taking the partial derivative with respect to each variable as follows:

$$\delta F(a,b) = \left\{ \left[\frac{\partial(F)}{\partial a}\right]^2 (\delta a)^2 + \left[\frac{\partial(F)}{\partial b}\right]^2 (\delta b)^2 \right\}^{1/2} \tag{A6}$$

By use of Eq. (A6) the standard deviations of the moduli and Poisson's ratio can be estimated by taking the partial derivatives of Eqs. (A1) through (A5) and evaluating them according to Eq. (A6). In doing this calculation, other equations can be derived:

$$\delta\nu = \left[\frac{V_L^2 V_G^4 (\delta V_L)^2 + V_G^2 V_L^4 (\delta V_G)^2}{(V_L^2 - V_G^2)^4}\right]^{1/2} \tag{A7}$$

$$\delta V_E = \left[\frac{(1 + \nu)(1 - 2\nu)(\delta V_L)^2}{1 - \nu} + \frac{V_L^2 \nu^2 (\nu - 2)^2 (\delta\nu)^2}{(1 - \nu)^3 (1 + \nu)(1 - 2\nu)}\right]^{1/2} \tag{A8}$$

$$\delta E = \left[\frac{4V_L^2 \rho^2 (1 + \nu)^2 (1 - 2\nu)^2 (\delta V_L)^2}{(1 - \nu)^2} + \frac{V_L^4 (1 + \nu)^2 (1 - 2\nu)^2 (\delta\rho)^2}{(1 - \nu)^2} + \frac{4\nu^2 (\nu - 2) V_L^4 \rho^2 (\delta\nu)^2}{(1 - \nu)^4}\right]^{1/2} \tag{A9}$$

$$\delta G = \left[4V_G^2 \rho^2 (\delta V_G)^2 + V_G^4 (\delta\rho)^2\right]^{1/2} \tag{A10}$$

$$\delta K = \left[\frac{(\delta E)^2}{9(1 - 2\nu)^2} + \frac{4E^2 (\delta\rho)^2}{9(1 - 2\nu)^4}\right]^{1/2} \tag{A11}$$

where

F = a function of a and b,
δF = the standard deviation of F,
δa = the standard deviation of a,
δb = the standard deviation of b,
V_L = the longitudinal velocity,
δV_L = the standard deviation of V_L,
V_G = the shear velocity,
δV_G = the standard deviation of V_G,
V_E = the extentional velocity,
δV_E = the standard deviation of V_E,
ν = Poisson's ratio,
$\delta\nu$ = the standard deviation of ν,
E = Young's modulus,

δE = the standard deviation of E,

G = the shear modulus,

δG = the standard deviation of G,

K = the bulk modulus,

δK = the standard deviation of K,

ρ = the sample density, and

$\delta\rho$ = the standard deviation of ρ.

The equations used to calculate the moduli and Poisson's ratio from wire data are different from the equations used for bulk samples since the extentional velocity, V_E, and torsional velocity, V_T, are measured (instead of longitudinal and shear). These equations are:

$$E = V_E{}^2\rho \ , \tag{A12}$$

$$G = V_T^2\rho \ , \tag{A13}$$

$$\nu = \frac{EY}{2G} - 1 \ , \tag{A14}$$

$$K = \frac{E}{3(1 - 2\nu)} \ , \tag{A15}$$

$$V_L = V_E\sqrt{\frac{1 - \nu}{(1 + \nu)(1 - 2\nu)}} \ , \tag{A16}$$

$$\delta E = \left[4V_E^2\rho^2(\delta V_E)^2 + V_E^4(\delta\rho)^2\right]^{1/2} \ , \tag{A17}$$

$$\delta G = \left[4V_T^2\rho^2(\delta V_T)^2 + V_T^4(\delta\rho)^2\right]^{1/2} \ , \tag{A18}$$

$$\delta\nu = \left[\frac{(\delta E)^2}{4G^2} + \frac{E^2(\delta G)^2}{4G^2}\right]^{1/2} \ , \tag{A19}$$

$$\delta K = \left[\frac{(\delta E)^2}{9(1 - 2\nu)^2} + \frac{4E^2(\delta\nu)^2}{9(1 - 2\nu)^4}\right]^{1/2} \text{, and} \tag{A20}$$

$$\delta V_L = \left[\frac{(1 - \nu)(\delta V_E)^2}{(1 + \nu)(1 - 2\nu)} + \frac{V_E{}^2\nu^2(\nu - 2)^2(\delta\nu)^2}{(1 - \nu)(1 + \nu)^3(1 - 2\nu)}\right]^{1/2} . \tag{A21}$$

To obtain an index of anistropy of the test materials, shear-velocity measurements were taken twice on the bulk pieces with the polarization direction rotated 90° between measurements. The standard deviation of the average shear velocity is calculated from:

$$\delta V_S = \left(\delta V_{G_0}^2 + \delta V_{G_{90}}^2\right)^{1/2} . \tag{A22}$$

The anistropy is calculated from:

$$A = \left(V_{G_0} - V_{G_{90}}\right)/2 \tag{A23}$$

APPENDIX B

RELATIONS BETWEEN ISOTROPIC ELASTIC CONSTANTS

Elastic Constants \ In Terms of	E, ν	E, G	B, ν	B, G	λ, μ
E	$= E$	$= E$	$= 3(1-2\nu)B$	$= \frac{9BG}{G+3B}$	$= \frac{\mu(3\lambda+2\mu)}{\lambda+\mu}$
ν	$= \nu$	$= -1 + \frac{E}{2G}$	$= \nu$	$= \frac{3B-2G}{2(3B+G)}$	$= \frac{\lambda}{2(\lambda+\mu)}$
G	$= \frac{E}{2(1+\nu)}$	$= G$	$= \frac{3(1-2\nu)B}{2(1+\nu)}$	$= G$	$= \mu$
B	$= \frac{E}{3(1-2\nu)}$	$= \frac{EG}{3(3G-E)}$	$= B$	$= B$	$= \lambda + \frac{2\mu}{3}$
λ	$= \frac{E\nu}{(1+\nu)(1-2\nu)}$	$= \frac{G(E-2G)}{3G-E}$	$= \frac{3B\nu}{1+\nu}$	$= B - \frac{2G}{3}$	$= \lambda$
μ	$= \frac{E}{2(1+\nu)}$	$= G$	$= \frac{3(1-2\nu)B}{2(1+\nu)}$	$= G$	$= \mu$

E = Young's modulus
ν = Poisson's ratio
G = Shear modulus
B = Bulk modulus (reciprocal of the compressibility)
μ, λ = Lamé constants

APPENDIX C

ELECTRICAL CIRCUITS OF THE WELDABLE RESISTANCE GAGES

The strain averaging circuit used in connection with the MG-425 resistance strain gages is shown in Fig. C1. Strain signals from the gages mounted on opposite sides of the specimen are added by the use of two full-bridge circuits placed in series. This corrects for specimen bending.

The gages, shown schematically in the inset, compensate for two sources of temperature error: (1) resistance change resulting from differential thermal expansion between the active gage filament and the test specimen, and (2) resistivity change in the active filament. The latter correction is made by incorporating a dummy filament inside the gage (see inset). Incorporating the dummy in the Wheatstone bridge as a leg adjoining the active filament and orienting its windings in the Poisson's plane cancels the effect of resistivity change and at the same time eliminates temperature-induced strain. The former correction is made by incorporating a low-ohm, fixed resistor (R_{TC}) in series with the active filament (R_a). Resistance R_{BAL} is added to give circuit stability.

A diagram of the circuit employed to treat strain signals for input into the plotters is shown in Fig. C2.

ORNL-DWG 78-9101

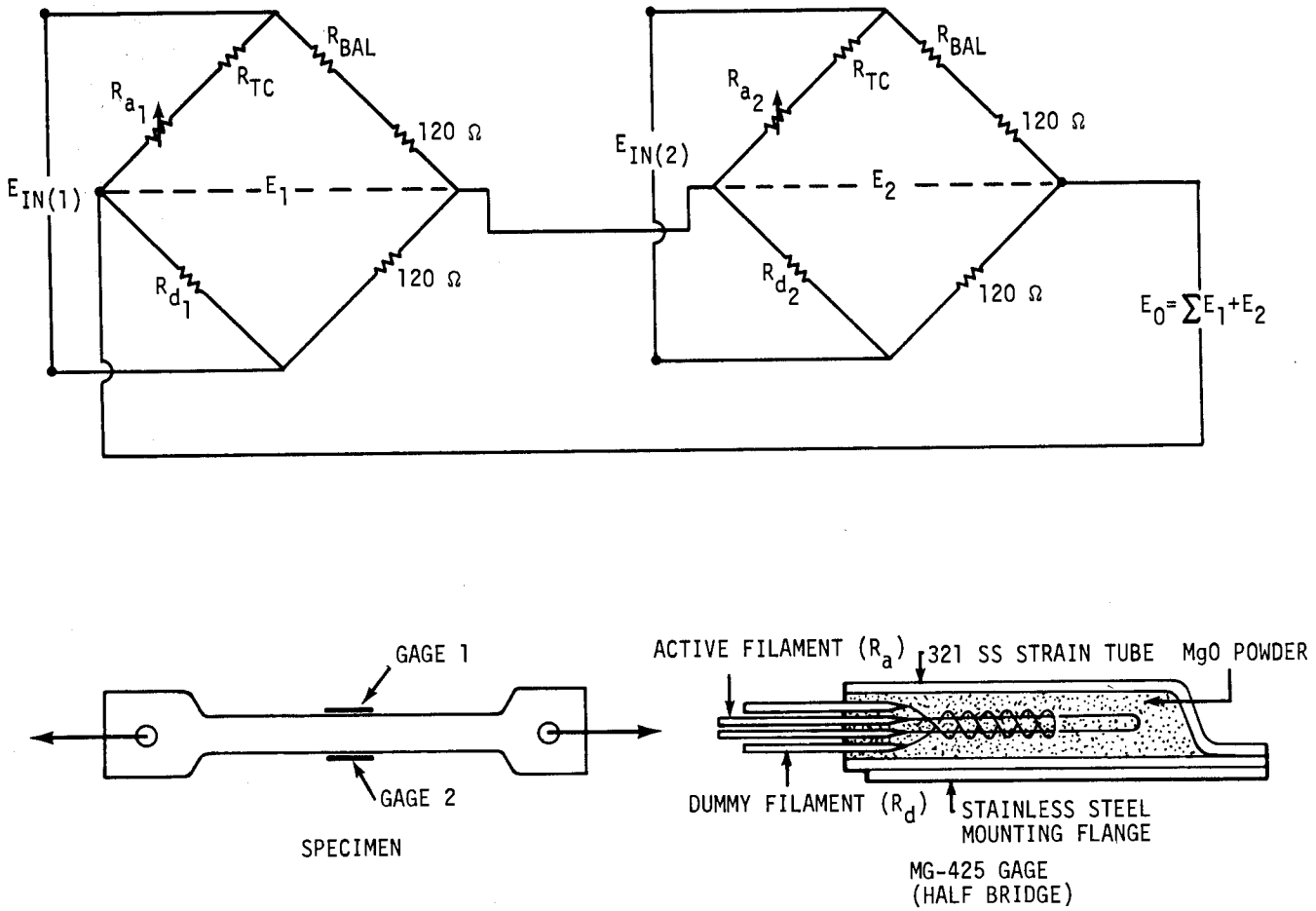

Fig. C1. Strain Averaging Circuit of Weldable Resistance Strain Gages. Adds two full-bridge outputs to cancel bending.

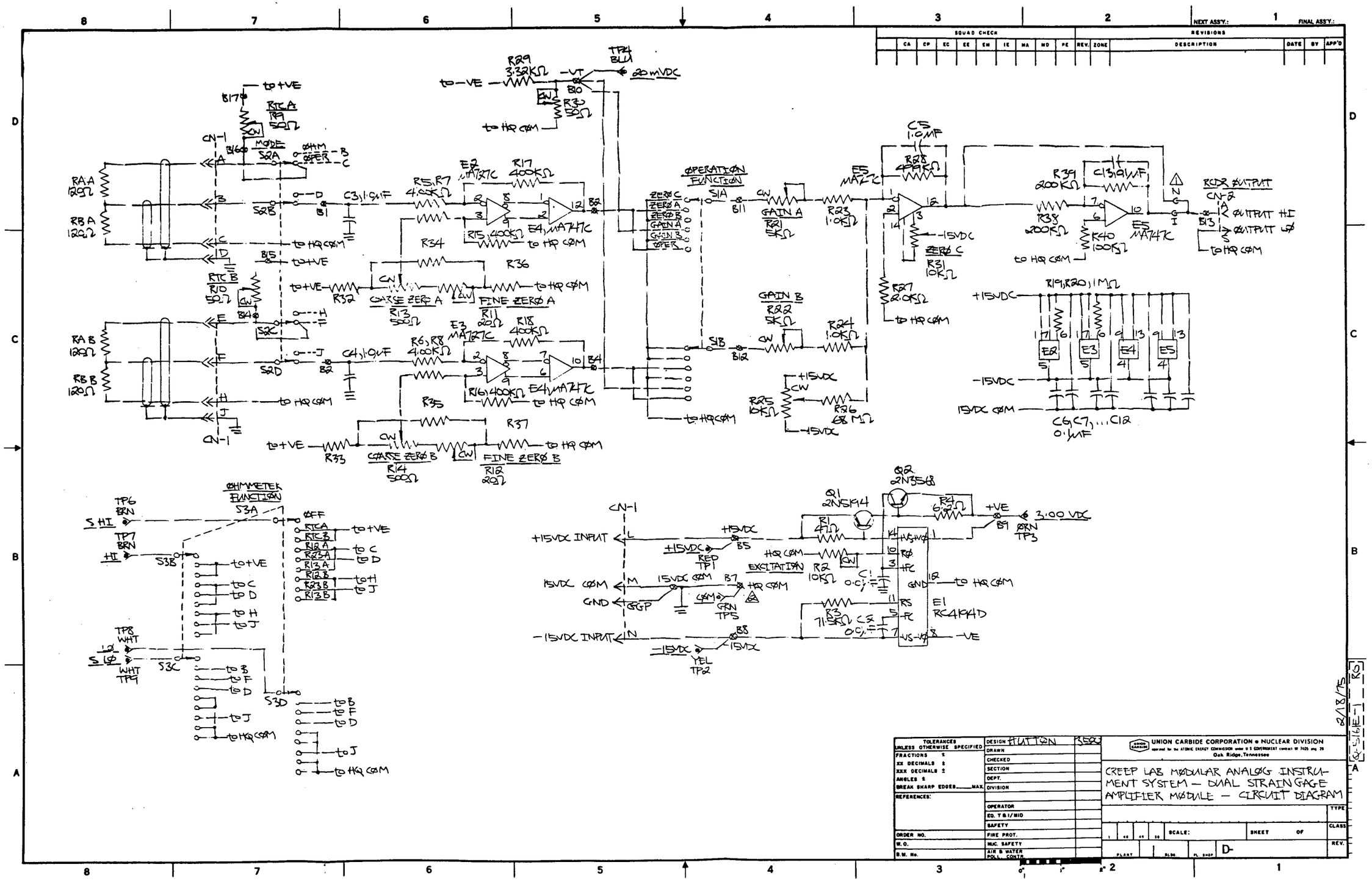

Fig. C2. Analog Circuit for Treating Weldable Resistance Strain Gage Signals.

ORNL-5442
Distribution
Category UC-79b, -h, -k

INTERNAL DISTRIBUTION

1-2. Central Research Library
3. Document Reference Section
4-5. Laboratory Records Department
6. Laboratory Records Department, RC
7. ORNL Patent Section
8. E. E. Bloom
9. M. K. Booker
10-14. C. R. Brinkman
15. J. M. Corum
16-20. J. R. Distefano
21-30. J. P. Hammond
31. R. F. Hibbs
32-33. M. R. Hill
34. J. F. King
35. R. L. Kluch
36. K. C. Liu
37. W. J. McAfie
38. R. W. McClung
39. H. W. McCoy
40. D. L. McElroy
41. J. W. McEnermey
42-46. M. W. Moyer (Y-12 Plant)
47-51. C. W. Nester, Jr.
52. C. E. Pugh
53-57. L. T. Ratcliff
58. V. K. Sikka
59. G. M. Slaughter
60. J. H. Smith
61. J. O. Stiegler
62. J. P. Strizak
63. R. W. Swindeman
64. G. T. Yahr
65. R. W. Balluffi (Consultant)
66. P. M. Brister (Consultant)
67. W. R. Hibbard, Jr. (Consultant)
68. M. J. Mayfield (Consultant)
69. N. E. Promisel (Consultant)
70. J. T. Stringer (Consultant)

EXTERNAL DISTRIBUTION

71-72. DOE Division of Reactor Research and Technology, Washington, DC 20545
73. Assistant Manager, Energy Research and Development, DOE-ORO
74-335. For distribution as shown in TID-4500 Distribution Category, UC-79b (Fuels and Materials Engineering Development); UC-79h (Structural Materials Design Engineering); UC-79k (Components)

☆U.S. GOVERNMENT PRINTING OFFICE: 1979-748-189/414